DEPARTMENT OF COMMERCE
FREDERICK H. MUELLER, Secretary

WEATHER BUREAU
F. W. REICHELDERFER, Chief

MONTHLY WEATHER REVIEW

JAMES E. CASKEY, JR., Editor

Volume 87
Number 10

OCTOBER 1959

Closed December 15, 1959
Issued January 15, 1960

AN OPERATIONAL OBJECTIVE ANALYSIS SYSTEM

GEORGE P. CRESSMAN
U.S. Weather Bureau, Washington, D.C.

[Manuscript received September 28 1959; revised November 25, 1959]

ABSTRACT

The system of objective weather map anaylsis used at the Joint Numerical Weather Prediction Unit is described. It is an integral part of the automatic data processing system, and is designed to operate with a minimum of manual supervision. The analysis method, based mainly on the method of Bergthórssen and Döös, is essentially a method of applying corrections to a first guess field. The corrections are determined from a comparison of the data with the interpolated value of the guess field at the observation point. For the analysis of the heights of a pressure surface the reported wind is taken into account in determining the lateral gradient of the correction to be applied. A series of scans of the field is made, each scan consisting of application of corrections on a smaller lateral scale than during the previous scan.

The analysis system is very flexible, and has been used to analyze many different types of variables. An example of horizontal divergence computed from a direct wind analysis is shown.

1. INTRODUCTION

The process of transforming data from observations at irregularly spaced points into data at the points of a regularly arranged grid has often been referred to as "objective analysis." An objective analysis scheme must perform several functions, namely, interpolation, removal of data errors, smoothing, and, in most applications, should contain some method of insuring internal consistency.

The method of analysis originally suggested by Panofsky [9] and modified to the system described by Gilchrist and Cressman [5], consisted of fitting some kind of polynomial by least squares to the data. Further efforts with this method were described by Cressman [4] and by Johnson [7]. This method, originally designed for areas of relatively dense and redundant data, did not prove too practical for use over a hemispheric area. Much of the hemispheric area is characterized by a few widely scattered observations, which one desires to fit as exactly as possible. The least squares polynomial scheme tended to develop instabilities of a certain type over such an area. Considerable effort was necessary to control these (Cressman [4]). Furthermore, the formation of the matrix elements and the matrix triangularization required at each grid point involved considerable computation. As a result of these considerations, the Joint Numerical Weather Prediction (JNWP) Unit, after extensive trials of the abovementioned scheme, changed its analysis procedure to the one described in the following sections. The system described below is based essentially on the general method described by Bergthórssen and Döös [2] and resembles to some extent the method recently reported by Haug [6].

2. PREPARATION OF THE DATA

One of the major problems in the practical application of any objective analysis scheme is the problem of data reliability and the detection and elimination of errors in the data. For this reason, a short description of the data preparation method follows.

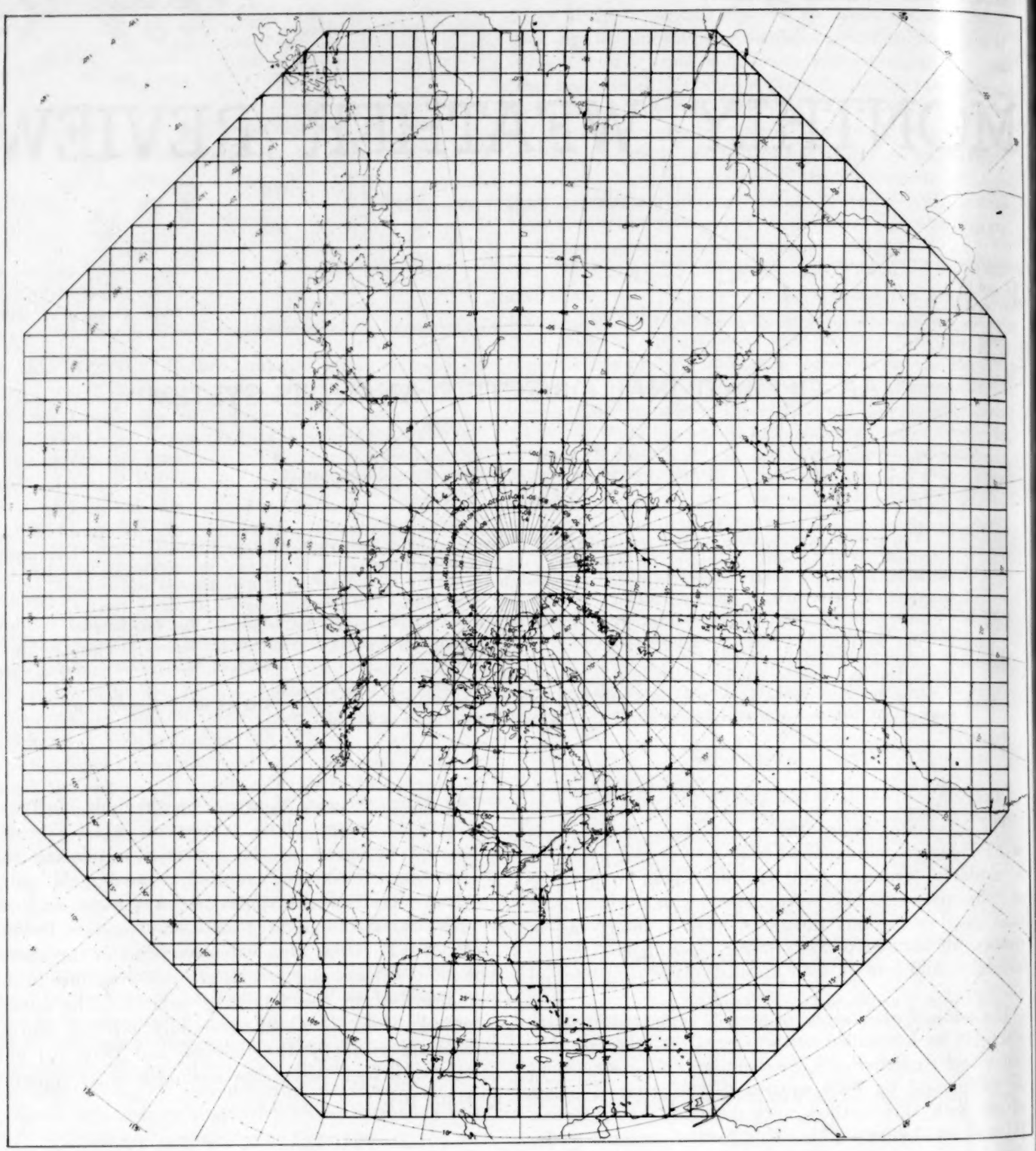

FIGURE 1.—The JNWP grid.

Data are received via teletypewriter from the Northern Hemisphere. The teletypewriter reports are processed automatically by an improved version of the automatic data processing system described by Bedient and Cressman [1], using the JNWP Unit's IBM 704 computer. During this process the temperature soundings are subjected to a hydrostatic check and corrected where possible. The erroneous data which cannot be corrected are deleted. All wind soundings are checked for vertical consistency, with the erroneous parts of the reports being deleted. The elements to be analyzed are then selected and sorted into a geographical order.

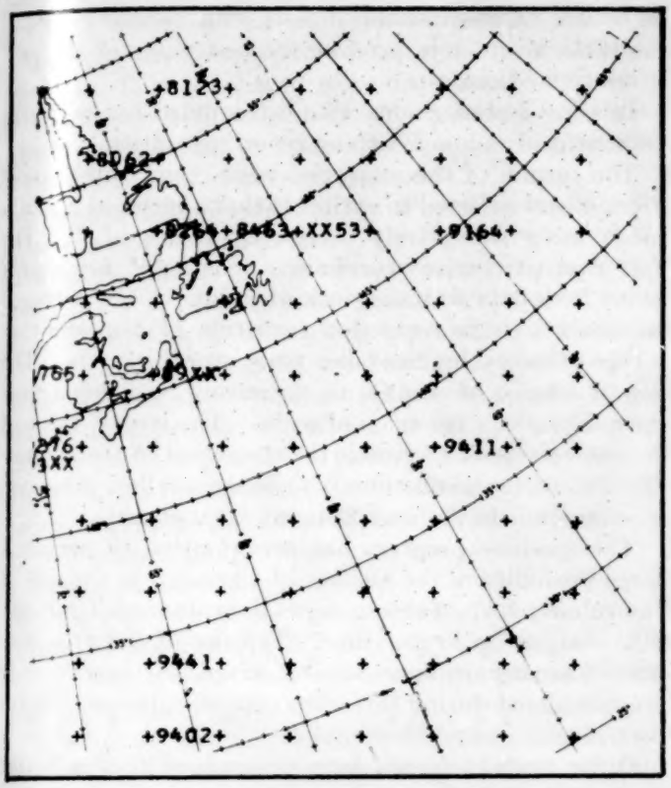

FIGURE 2.—Section of a plotted chart. The two left-hand digits are the thousands and hundreds digits of the 500-mb. height. The third digit is the wind direction on an eight point scale (0 = North), and the fourth digit is the wind speed in tens of knots. Missing data are indicated by X's.

At this point a control on the process is introduced by means of the production of a plotted chart. Here, the digits of highest significance are printed in their approximate geographical location (within the nearest grid square). The grid currently used for analysis and forecasting is shown in figure 1. A section of the plotted map is shown in figure 2. This plotted map gives the monitoring analyst a picture of the data coverage. The listing of each report on the map is also helpful for subsequent monitoring of the automatic error rejection process. The plotted map is quite cheap to obtain, requiring 10 seconds for the calculations and the preparation of the tape, which is then used to print the map on the off-line printer. The printing requires about 40 seconds.

TABLE 1.—*The type of first guess used for each type of analysis*

Field analyzed	First guess
500-mb. height	12-hr. forecast.
850-mb. height	Current 500-mb. chart minus forecast 850–500-mb. thickness.
300-mb. height	Estimated 300-mb. chart obtained by vertical extrapolation from 850 mb. and 500 mb.
700-mb. temperature	700-mb. temperature estimate obtained by relabeling current 850–500-mb. thickness chart.
700-mb. dewpoint depression	24-hr. forecast, if available, otherwise a constant average value.
u and v components of the wind	Geostrophic u and v components.

(All forecasts are from numerical models now in use at JNWP)

3. THE ANALYSIS SCHEME

The analysis scheme has been designed to have a maximum of flexibility, and has been used for the analysis of many different elements. The method consists essentially of using the reported data to make successive corrections to an initial guess. Suitable smoothing routines are interspersed.

In order to obtain the greatest amount of accuracy with the least amount of computation, it is essential that the first guess be as accurate an approximation to the final field as possible. Table 1 lists some of the various types of analysis which have been performed together with the first guess which was used. The choice of a first guess is in some cases arbitrary, but can easily be changed if a better guess can be obtained by some other means. The use of a forecast of any element as a first guess for the analysis at a subsequent time would involve complications from boundary errors if the forecast and analysis grid were of much smaller size than that shown in figure 1.

The analysis is then performed in a series of "scans"; i.e., passes through the field. In a given scan, the grid points are considered successively. The values of the first guess of the element to be analyzed are corrected according to the reported data. In order to illustrate the correction process, the analysis of 500-mb. heights from mixed wind and height data will be considered.

If height only is reported by an observing station, a correction C_h is computed for a nearby grid point, as given by the relation

$$C_h = -WE_h \tag{1}$$

where E_h is the error of the interpolated value of the first guess field at the location of the observation, and W is a weighting factor given by

$$W = \frac{N^2 - d^2}{N^2 + d^2}. \tag{2}$$

In the expression for W, d is the distance between the grid point and the observation, and N is the distance at which W goes to zero (only positive values of W are used). The curve of W vs. d is shown in figure 3. The simplified form for W, as compared to that used by Bergthórssen and Döös, or as compared to some suggestions received, was chosen in order to minimize the amount of computing required. The weighting factor, depending on the distance d, must be computed a very large number of times in each scan, and the computation time must be kept short. Since N^2 is fixed for a given scan, the computation of a value of W involves one each multiplication, subtraction, addition, and division, and is economical.

If both a height and a wind are reported, a correction C_v is computed for a nearby grid point, as given by

$$C_v = W\left[D_v + \frac{kf}{mg}(v\Delta x - u\Delta y) - D_g\right] \tag{3}$$

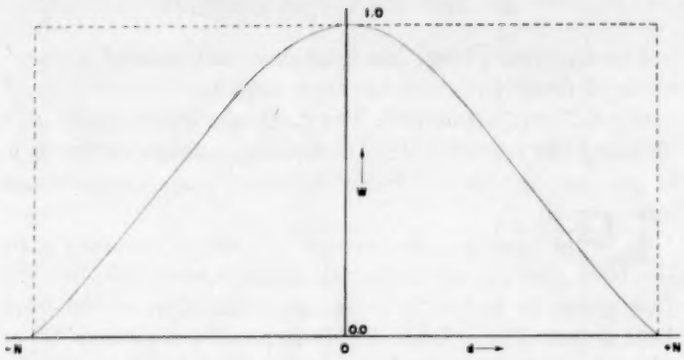

FIGURE 3.—Curve of the weighting function W vs. distance d. Solid line refers to equation (2). Dashed line refers to recent changes for scan 4 (see text).

Where D_o is the observed height at the location of the observation, u and v are the observed wind components in the x and y directions at the same point, f is the Coriolis parameter, g is the acceleration of gravity, m is the map scale factor, Δx and Δy are the components of the map distance from the observing point to the grid point, and D_g is the value of the height at the grid point in the first guess. The factor k represents the average ratio of the geostrophic to the actual wind, and is set at 1.08 (see [8]). This amounts to passing a plane in the xyz coordinates through the observation, multiplying the increment between this plane and the first guess of the pressure surface by W, and adding the resulting increment to the first guess.

If only a wind is reported, C_v is determined by equation (3) except that D_o is then the height interpolated from the first guess at the location of the observation.

All the data within the radius N of the grid point under consideration are considered. Each observation reporting a height is used in the computation of a value of C_h, and each observation reporting a wind is used in computing a value of C_v. Thus for a station reporting both height and wind there is a value of C_h and a value of C_v. After the values of C_h and C_v have been computed, the correction C to be applied is determined as a weighted mean; i.e.,

$$C=\frac{A\Sigma C_h+\Sigma C_v}{An_h+n_v}, \tag{4}$$

where n_h and n_v are the numbers of C_h and C_v values respectively, and A is a weighting factor. The factor A can be regarded as the weight given to the lateral gradients of the first guess as compared to the observed winds, which have a weight of one, and is given the value of ¼. The value given to A naturally depends on the quality of the lateral gradients of the first guess. For example, in the computation of 100-mb. analyses, the first guess is taken as the chart for the previous time. Since it is desired to fit the observed winds quite closely, A is taken to be 2^{-5}. A short series of tests with various values is desirable in order to produce the best value of A for a given type of analysis.

In a given scan, a correction is computed for each grid point within radius N of any reporting station.

The feature of this analysis scheme which differs most from others referred to earlier is that a series of scans is made using successively decreasing values of N. The fact that the various corrections (computed for a grid point from data with the circle of radius N) are averaged to obtain a single correction (equation (4)) means that a type of smoothing has taken place over this circle. The use of a series of scans with decreasing N values allows the analysis of a spectrum of scales. The largest value of N used can be set to permit the correction of the largest-scale errors in the first guess, while the smallest value sets a lower limit to the scale that can be analyzed.

The machine program has been written to permit a large flexibility in the number of scans and in the size of the values of N. Table 2 shows the values used for 500-mb. analysis up to this time. The size of the area considered during the first scan is so large that heights only are considered during this scan. On all subsequent scans both heights and winds are used.

Quite recently it has been determined that a better horizontal resolution of the smaller-scale components of the 500-mb. height field can be obtained by modification of the weighting factor used during the last scan to a constant value of 1.00 from the observation location out to the distance N, where it becomes zero. The value of N for the fourth scan is set at 1.00 grid lengths. This revised weighting factor is indicated by the dashed line in figure 3.

Early trials with the analysis indicated that in an area where the first guess was very poor, slight discontinuities tended to develop at a distance of 3 to 4 grid lengths from an isolated observation; i.e., at the distance where the weighting factor is rapidly approaching zero. This was corrected economically by the introduction of a smoothing program. This program makes passes of the field D using the smoothing function

$$\overline{D}=\tfrac{1}{2}D+\tfrac{1}{8}\Sigma D \tag{5}$$

where ΣD refers to the sum of the values of D at the four nearest grid points. During a 500-mb. analysis the smoothing is done one time between scans 2 and 3 and one time between scans 3 and 4.

In an operational system where a forecast from a previous analysis is used as a first guess for the next anal-

TABLE 2.—*Values of N corresponding to successive scans.*

Scan No.	N (grid lengths)
1	4.75
2	3.60
3	2.20
4	1.80

ysis, the above smoothing has the additional function of gradually reducing the amplitude of smaller-scale systems which continually remain in areas of very little or no data. This is believed to be a desirable attribute of the system, since there is no known method of forecasting which permits an accurate description of small-scale systems a number of days in advance.

Since the 500-mb. height field is used as input to the balance equation (Shuman [11]) the conclusion of the analysis is used as an opportunity to apply the restriction $\zeta_g > -f/2$, where ζ_g is the geostrophic relative vorticity. This is done by making successive modifications of the height field until the required criterion exists. When applied at 500 mb. and at lower levels this usually results in modifications of the height field which are smaller than the probable errors of the observations. At higher levels this seems at times to be an unrealistic criterion to apply, since the required height changes can greatly exceed the probable data errors.

Finally, a smoothing is applied to the height field with the use of a smoothing operator (Shuman [12]) which eliminates components of wavelength of 2 grid units, while leaving those of 5 or more grid units wavelength practically unchanged.

The results are printed in two forms. First is the printed 500-mb. chart. Following this, a chart is printed showing the difference between the final result and the first guess. This latter chart is useful in monitoring, and for detection of special errors and any unusual problems which may arise.

4. AUTOMATIC ERROR DETECTION AND REMOVAL

Errors of all sizes can still occur in the data furnished to the analysis program. The checks for vertical and internal consistency as well as the comparison of duplicating reports made in the pre-analysis processing do not remove all errors. For example, there may be a partially garbled report which was too damaged to permit the usual checks. The remaining data could contain an error.

As mentioned earlier, it is necessary to obtain an interpolated value of the height field of the previous scan or guess field at the location of an observation before making the next scan. At the same time an interpolated value of the geostrophic wind is computed. Before each scan, a comparison is made between the interpolated and reported winds and heights. If the difference exceeds a certain value, the reported value is rejected and erased from the memory of the computer. The limits set as rejection criteria are listed in table 3. As a last check the stations whose reports deviate from the final analysis by more than 200 ft. or 40 knots are listed for the information of the monitoring analyst.

When data are selected for rejection by the above process, the location of the reporting station is listed on the printer, together with the type of rejection. If the monitoring analyst chooses, he can cause the computer to stop after each data listing. By the use of certain switches, he can cause the listed data to be rejected or retained and used, as he wishes. However, ordinarily all listed data are rejected.

TABLE 3.—*Maximum permissible difference between data and the interpolated field values of the previous scan for 500 mb.*

Prior to scan No.—	Height difference	Vector wind difference
	Feet	*Knots*
1	700	90
2	600	70
3	500	70
4	350	60

The use of successively decreasing error limits as shown in table 3 represents a gradual tightening up of the error toleration as the analysis is refined by successive iterations. Observations differing unreasonably from the first guess are rejected immediately before scan 1. Observations differing excessively from their neighbors are rejected later. As an average number, about two or three reports are rejected during the course of a hemispheric analysis, in which 400 to 500 reporting stations are used. Naturally, there are many more errors in the data than two or three, but the majority are removed or corrected in the pre-analysis processing.

5. OPERATIONAL USE OF THE ANALYSIS PROGRAM

The total time required on the IBM 704 computer for a 500-mb. analysis over the grid of figure 1 averages about 15 minutes, with some variation depending on the amount of data received. All maps are printed on the off-line printer, requiring the additional time of 3 minutes each for the last two maps. The time required for the 850-mb. analysis is about the same. An analysis of dewpoint depression has been done 3 times weekly for experimental quantitative precipitation forecasts and requires only about 9 minutes, since experience has shown that fewer iterations of this analysis are required. Maps of any single field for the United States area require a total of 6 minutes, since this occupies only a small fraction of the total grid area. The time of 6 minutes represents almost an irreducible minimum with the present program due to the required overhead of sorting, tape handling, etc.

The 500-mb. analysis has been done by computer at the JNWP Unit every 12 hours for 1½ years, starting in early April 1958. Since that time no hand analyses have been made. The 850-mb. analysis has been done by computer for over a year, starting in late summer of 1958. The only manual interventions required come in the form of additional reports, sometimes synthetic, which are introduced by the monitoring analyst.

For the 500-mb. analysis, the additional reports are of four types. The first represents a hand-editing of reports from non-reconnaissance aircraft. These reports, in so-called plain language, are at the present time too unsystematic in form and doubtful in accuracy to be

edited automatically. The second type represents a vertical extrapolation of surface data to 500 mb. This is done occasionally in areas of surface but no upper air data, especially when it is thought that a failure might occur in the 12-hr. forecast because of sudden cyclogenesis. The third type is entered in certain areas where the data are always received too late for current use (more than 6¼ hr. after observation time). In such areas selected pieces of the late data are modified by the 12-hr. forecast and entered as current data on the next map. The Siberian Arctic coast is one area where such steps are necessary. Finally, there are always some reports which are received too badly garbled for machine recognition. These are indicated on the monitoring list provided by the automatic data processing program. In some of these cases, the monitoring analyst can retrieve the 500-mb. data and enter them by hand.

For the 850-mb. analysis a number of surface ship reports are entered by hand for oceanic areas of sparse upper air data. These are automatically extrapolated by the computer to 850 mb. These must be entered by hand due to the large frequency of errors in the ship position reports, which makes automatic editing risky. In principle one can handle this problem automatically by simulating the manual procedures; i.e., by keeping a running log of several days on the position of the ships and by correcting the erroneous position reports. However, the problem is complicated by the lack of identification of many ships and by errors in the identification of others. Nevertheless, we plan to attempt to program a system of this type before long.

It can be seen that most of the hand entering of data is necessitated by imperfections of the meteorological reporting and communication methods; i.e., by slow or inaccurate communications from remote areas and by insufficient checking information in the reports. In time these situations may improve, permitting increased automation.

6. GEOSTROPHIC AND NON-GEOSTROPHIC ANALYSIS

The analysis scheme described above, when used for analysis of the height of a pressure surface, needs a specification of the relation between the wind and the height gradient. In equation (3), this is specified as being essentially geostrophic. However, it is important to note that this specification applies less and less strictly as one goes farther from an observing station, with the result that the final analysis is not necessarily very geostrophic. The departures from geostrophic winds shown in the analysis can be considerable in an area of high observation density where the reported winds and heights do not agree well with the geostrophic approximation.

In [4] an analysis experiment was described in which the wind relation used was given by the balance equation; i.e.,

$$\nabla^2\psi=\frac{1}{f}\left\{\nabla^2\phi+2\left[\left(\frac{\partial^2\psi}{\partial x\partial y}\right)^2-\frac{\partial^2\psi}{\partial x^2}\frac{\partial^2\psi}{\partial y^2}\right]-\nabla\psi\cdot\nabla f\right\}, \quad (6)$$

and

$$u=-\frac{\partial\psi}{\partial y},\ v=\frac{\partial\psi}{\partial x}, \quad (7)$$

where ϕ is the height of the pressure surface and ψ is the stream function.

An analogous experiment was performed with the analysis program described in this paper, with the use of the following procedure:

(a) Using a 24-hour forecast as first guess (for consistency with the other examples shown below) the 500-mb. height analysis was made using heights only. Reported winds were not considered.

(b) Equation (6) was solved for a stream function map, using the heights of (a) as input data.

(c) Using the stream function map of (b) as first guess, an analysis was made using only the reported winds. For this purpose equation (3) was changed to

$$C_v=W\left[\psi_o+\frac{1}{m}\left(v\Delta x-u\Delta y\right)-\psi_g\right] \quad (8)$$

The symbols have the meanings given previously except that ψ_o and ψ_g are the stream functions of the first guess at the observation point and the grid point, respectively.

(d) Given values of ψ, equation (6) was solved for the height field.

Insufficient analyses of this type have been done to show any pronounced differences between nongeostrophic and geostrophic analyses. However, it is probable that the inaccuracies arising in the solution of a Poisson equation over a large (1,977 points) grid make the accurate representation of the final heights of the pressure surface extremely difficult. This conclusion is supported by the examples given in the next section.

7. EXAMPLES

Several experiments were made with the data for 0000 GMT, August 20, 1959. For convenience in representation, the analyses were confined to the area shown in figure 4. In order to make the examples more interesting, a 24-hour forecast was used as the first guess instead of the usual 12-hour forecast. Analyses were conducted with the following variations:

(a) A complete 500-mb. analysis.

(b) An analysis using the reported heights only and disregarding the reported winds.

(c) An analysis using the reported winds only and disregarding the reported heights.

(d) An analysis using the balance equation as the wind law.

Verifications of the analyses were made by computing the r.m.s. difference between the reported heights and

the heights interpolated from the analyses to the locations of each observation. The interpolation was made in the plane fit by least-squares to the four heights at the corners of the grid square containing the observations. The r.m.s. vector wind difference between reported winds and geostrophic winds from the analyses was also computed for each map. The interpolation in the analysis was made linearly in each grid square. In the case of the non-geostrophic analyses, the wind relation of equation (7) was used. The results are given in table 4. Figure 4 shows the height analysis obtained by item (2) in table 4, together with the data used.

One of the most interesting results shown in table 4 is the excellent quality of the analysis obtained when using only the reported winds. In an analysis for winds only, the mean height over the area is not changed. If the area analyzed is large enough that the mean algebraic height error of the first guess is very small, the heights of the resulting analysis will be accurate. So far as this example is representative, one could conclude that most of the information regarding the 500-mb. contours in a dense data area is contained in the winds, the heights being relatively redundant information.

Even in an area of dense data the results of this analysis scheme are not completely independent of the first guess. The slightly lower height error obtained with the 24-hour forecast as first guess as compared with the 12-hour forecast is probably attributable to the apparent diurnal variations of the 500-mb. surface.

8. DIRECT WIND ANALYSIS

An analysis of the u and v components of the wind can be made by the above method by obtaining a first guess of the components of the wind from a stream function map. Then by using the correction equation (1) and by going through a series of scans, as described earlier, a separate analysis of each wind component can be obtained. This adaptation of the analysis program was made by Mr. A. Kneer and Capt. J. Neilon, USAF, of the JNWP Unit, who made several such analyses. The divergence field computed from one of these analyses is shown in figure 5.

Referring to figure 4, we can see that the divergence field of figure 5 is relatively smooth and has believable magnitudes in areas of dense wind coverage. In other areas, the magnitudes seem suspiciously large for 500 mb. in a summer situation. For example, the wind at Churchill, Manitoba, seems to be considerably subgeostrophic on figure 4, and is largely responsible for the relatively strong convergence and divergence patterns indicated to the west and east of that station. The reality of this situation is difficult to estimate without additional supporting data.

Variations in the analysis procedure were tried, but did not effect changes in the divergence of more than 20 percent. It is therefore concluded that the divergence pattern of figure 5, over the United States, is indicated by

TABLE 4.—*Comparison of analyzed values and the data for experiments on August 20, 1959, 0000 GMT.*

	r.m.s. height error (meters)	r.m.s. wind error (meters/sec.)
(1) 24-hr. forecast	35.3	7.0
(2) height and winds used: 24-hr. forecast as 1st guess	14.0	5.2
(3) heights only: 24-hr. forecast as 1st guess	18.2	6.0
(4) winds only: 24-hr. forecast as 1st guess	14.6	5.2
(5) non-geostrophic analysis	17.8	5.2
(6) heights and winds used: 12-hr. forecast as 1st guess	16.2	4.9

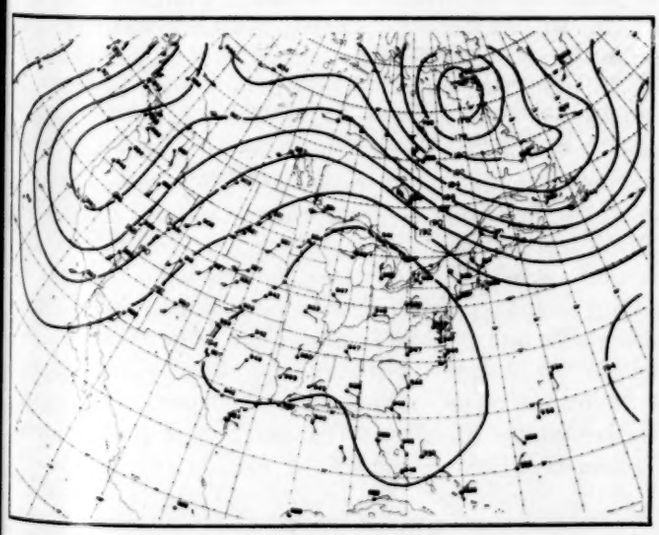

FIGURE 4.—Objective analysis for a North American section of the map for 0000 GMT, August 20, 1959. The contours were traced from the band-contour output of the IBM 717 printer.

FIGURE 5.—Horizontal divergence computed from a direct wind field analysis. Values are in units of 10^{-6} sec.$^{-1}$. Map for 500 mb., 0000 GMT, August 20, 1959.

the observed winds, and does not depend very much on the details of the analysis procedure. Further studies will be made of divergence patterns using this method of analysis.

9. THE PROBLEM OF INTERNAL CONSISTENCY

The internal consistency required of an analysis system depends on the use to be made of the analysis. Since direct wind-field analysis over a large part of the hemisphere does not seem feasible with today's data, forecast models of the next few years will probably have to use the height field and its derivatives as input data. A procedure suitable for currently-used multi-level models has been to use the first two surfaces analyzed in an extrapolation to the other levels (see Brown [3]). This extrapolation is used as the first guess, and is modified only by reported data. However, this method still does not insure that the implied static stability will everywhere remain positive if the surfaces analyzed are close together in the vertical. For this problem it is planned to use a special program which makes the necessary small adjustments in the heights of the pressure surfaces to insure positive stabilities everywhere.

10. CONCLUSIONS

The analysis system described above has proven to be a flexible, inexpensive, and satisfactory system for the present requirements of numerical prediction, and has been in continuous operational use for over a year.

For more advanced prediction models, particularly those using the "primitive" equations of motion, the demands for internal consistency may exceed the capabilities of this system. Suggestions for more elegant methods of achieving internal consistency have been made by Sasaki [10].

The problem of automatic recognition and correction or removal of erroneous data is a very urgent one. The methods described in this paper have worked fairly well in operational use. However, a much more satisfactory solution would involve improved methods of automatic detection and correction of the communication errors directly on the circuits, since these account for the majority of the "erroneous" reports.

ACKNOWLEDGMENTS

The assistance of Mr. A. Kneer, U.S. Weather Bureau, who programmed the initial sorting and conversion of data, and of Capt. J. Neilon, USAF, who programmed the adaption for direct wind analysis is gratefully acknowledged.

REFERENCES

1. H. A. Bedient and G. P. Cressman, "An Experiment in Automatic Data Processing," *Monthly Weather Review*, vol. 85, No. 10, Oct. 1957, pp. 333–340.
2. P. Bergthórssen and B. Döös, "Numerical Weather Map Analysis," *Tellus*, vol. 7, No. 3, Aug. 1955, pp. 329–340.
3. J. A. Brown, "Multiple Linear Regression Equations Expressing Heights of Certain Pressure Surfaces," Technical Memorandum No. 15, Joint Numerical Weather Prediction Unit, April 1959, 5 pp.
4. G. P. Cressman, "An Objective Analysis Study," Technical Memorandum No. 12, Joint Numerical Weather Prediction Unit, June 1957, 12 pp.
5. B. Gilchrist and G. P. Cressman, "An Experiment in Objective Analysis," *Tellus*, vol. 6, No. 4, Nov. 1954, pp. 309–318.
6. O. Haug, "A Method for Numerical Weather Map Analysis," *Scientific Report*, No. 5, Det Norske Meteorologiske Institutt, 1959, 10 pp.
7. D. H. Johnson, "Preliminary Research in Objective Analysis," *Tellus*, vol. 9, No. 3, Aug. 1957, pp. 316–322.
8. M. Neiburger, T. Sherman, W. W. Kellogg, and A. F. Gustafson, "On the Computation of Wind From Pressure Data," *Journal of Meteorology*, vol. 5, No. 3, June 1948, pp. 87–92.
9. H. A. Panofsky, "Objective Weather Map Analysis," *Journal of Meteorology*, vol. 6, No. 6, Dec. 1949, pp. 386–392.
10. Y. Sasaki, "An Objective Analysis Based on the Variational Method," *Journal of Meteorological Society of Japan*, Series II, vol. 36, No. 3, June 1958, pp. 77–88.
11. F. G. Shuman, "Numerical Methods in Weather Prediction: I. The Balance Equation," *Monthly Weather Review*, vol. 85, No. 10, Oct. 1957, pp. 329–332.
12. F. G. Shuman, "Numerical Methods in Weather Prediction: II. Smoothing and Filtering," *Monthly Weather Review*, vol. 85, No. 11, Nov. 1957, pp. 357–361.

FORECASTING MIDDLE CLOUDINESS AND PRECIPITATION AREAS BY NUMERICAL METHODS

LIEUTENANT COMMANDER EDWARD M. CARLSTEAD, USN

Fleet Weather Central, Suitland, Washington 25, D.C.*

[Manuscript received July 9, 1959; revised October 7, 1959]

ABSTRACT

A numerical prediction model suitable for computation using large-scale digital computers to forecast amounts of middle cloudiness, areas of precipitation, and precipitation amounts is presented. The model described uses products derived from an operational Joint Numerical Prediction Unit forecast model. Background information, certain mathematical equations, and input-output format are presented. Figures showing a sample series of prognostic charts are presented. Results, limitations, and future prospects are discussed.

1. BACKGROUND

The providing of upper-level and surface prognostic charts for use in the field has been undertaken with considerable success by many meteorological activities including the Joint Numerical Weather Prediction Unit (JNWP) and the National Weather Analysis Center (NAWAC). The increasing success of these products serves to remind one of the other "face" of the prognostic "coin," namely, determining weather elements from prognostic information. This paper describes a beginning method of predicting areas of occurrence of middle cloudiness including amounts, and areas of large-scale precipitation including quantitative amounts. Further, these predictions will be produced in a form suitable for transmission to field activities for operational use.

Work has been done on this problem in the past. Smagorinsky and Collins [5] considered the problem of the mechanics of the formation of precipitation based on the laws of fluid mechanics and used a computer to solve these laws in the form of certain mathematical equations. With the placing in operation of the "thermotropic" two-level model at JNWP in the spring of 1956 [7], charts of initial and forecast vertical motions were made available. Coincident with this, studies were commenced at JNWP to examine some possible uses for these charts. One result of this examination was the development of a technique by Lewis [4] using vertical motions and constructed 700-mb. trajectories to forecast the change in the 700-mb. dewpoint depression at one station for a period of 36 hours. This work showed the difficulty of numerically forecasting the change in 700-mb. dewpoint depression unless both horizontal advection and changes due to vertical motion were considered. Another result of this work was the determination of a nomogram (fig. 1) of the relationship between middle cloudiness, precipitation, vertical motion, and 700-mb. dewpoint depression. The sample of data going into this scatter diagram was fairly small, but additional samples of data have tended to confirm the isolines of the nomogram. The promising results of Lewis' work led to a project at JNWP to adapt this technique to a hemispheric grid and to compute a forecast of a field of dewpoint depressions and associated weather patterns by use of the high-speed IBM 704 computer at JNWP in Suitland, Md.

2. INITIAL MOISTURE INPUT FIELD

The moisture that is contained within the atmosphere is distributed irregularly through it. It would be desirable to attempt to forecast the changes in moisture at many levels within the atmosphere. However, because of the limitations in the number of fields that can be carried internally within the machine, it is not possible to treat more than one level at present. It was decided to work with the advection of moisture at 700 mb. because this would allow the direct usage of the results of Lewis' work; because the 700-mb. level is near the primary level (500 mb.) of the present operational JNWP models; and finally, because the presence of moisture at 700 mb. is a good indicator of a "deep" moisture layer. Upon examination of early forecasts it was seen that several forecasts were "missed" because the atmosphere was saturated from the ground to just below the 700-mb. level and was very dry above. This caused the model to work with a much too dry moisture field. It was decided to modify the moisture input data by computing a moisture field consisting of the average of the 850-mb. and 700-mb. dewpoint de-

*Work undertaken while assigned to the Joint Numerical Weather Prediction Unit, National Meteorological Center. Present affiliation: U.S. Navy Project NANWEP, U.S. Navy Postgraduate School, Monterey, Calif. Opinions expressed by the author are his own and do not necessarily reflect the views of the Navy Department.

532363—60——2

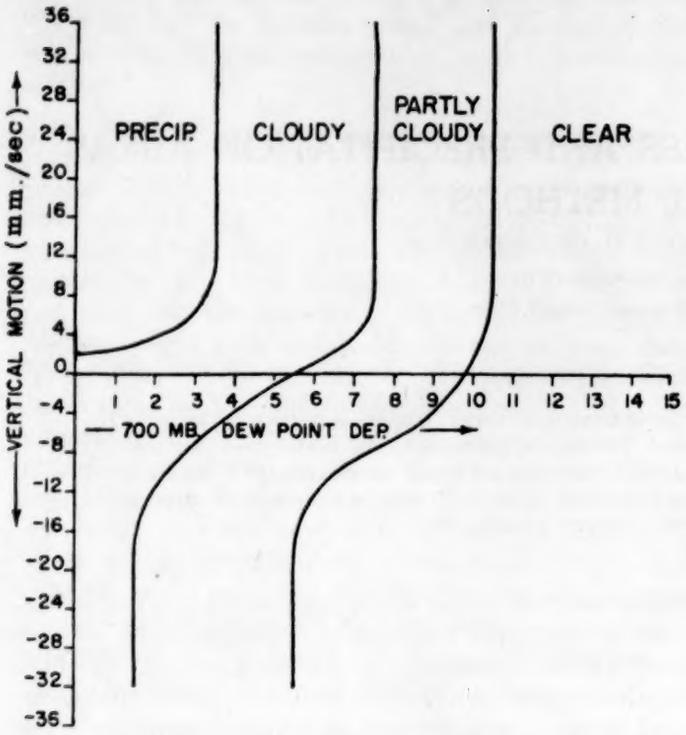

FIGURE 1.—Nomogram used for determination of weather categories, giving weather as a function of vertical motion in millimeters per second and the 700-mb. dewpoint depression in degrees Celsius. Enter nomogram with 700-mb. dewpoint depression and vertical motion and forecast weather indicated within envelopes. (From [4].)

pressions. This resulted in an immediate improvement in forecasts. Another data problem encountered was due to the scarcity of moisture data aloft over the ocean areas of the world. This problem can be reduced considerably by inferring the 850–700-mb. dewpoint depression from surface ship reports. Referring to the nomogram (fig. 1) it can be seen that if certain weather conditions (say, rain) are observed, a dewpoint depression of about 2° C. can be assumed without too much error. This type of inferred report is easily introduced into the automatic data processing system [1] that is currently operational at JNWP.

The operation begins with the analysis of the initial moisture field. Data for the analysis are obtained from the automatic data processing data tapes. The analysis is performed by the JNWP objective analysis program. This analysis program starts with a "guess" field consisting of the 24-hour forecast dewpoint depression field available from the previous day's run and modifies this guess field with current data. This technique has the valuable attribute of preserving continuity over areas of sparse data. The output of the analysis program consists of a map of dewpoint depressions, a coverage chart of stations reporting data, a chart of the difference between the "guess" (24-hour forecast) field and the final analysis (hence providing, among other things, a verification of the 24-hour forecast dewpoint depressions), and a punched card deck, in binary, of the dewpoint depression field.

3. FORECASTING MODEL

The forecasting model, which uses the moisture field which was obtained as described in the previous section, depends upon the hourly fields of 500-mb. stream function data, $\hat{\psi}_5$, the hourly large-scale vertical motions, ω, and the hourly forecast 850–500-mb. height thickness fields, Δz, all of which are saved on a magnetic tape from the operational run of the JNWP two-level model. The general principle of operation of the middle cloud and precipitation area forecast is to advect the initial moisture field with a computed 700-mb. stream field, modifying the dewpoint depression with the forecast vertical motions. Then, with the aid of the Lewis nomogram, the expected future weather conditions can be determined from the forecast moisture field and the forecast vertical motion field. To obtain the wind velocity at 700 mb. the following interpolation is performed:

$$\hat{\psi}_{7i,j}=\hat{\psi}_{5i,j}-\alpha\Delta z_{8.5-5i,j},$$

where

$$\alpha=\left(\frac{z_5-z_7}{z_5-z_{8.5}}\right)_{\text{Std. Atm.}} \tag{1}$$

In interpolating for the wind at 700 mb., the wind is assumed to vary linearly with height, and the shear wind is assumed to be reduced below the geostrophic by the factor $f/\bar{f}$, where $\bar{f}$ is the Coriolis parameter at 45° of latitude. The geostrophic wind shear was first used, but it was found to yield much too large wind speeds in low latitudes. No serious error is caused in middle latitudes or even in high latitudes by replacing f by $\bar{f}$ in the expression for shear wind, and more realistic, if not more accurate, wind values are obtained in low latitudes. In the solution of the balance equation at JNWP to obtain stream function values, z is used as the boundary value for $(\bar{f}\psi)/g$. This not only reduces the velocity normal to the boundary below the geostrophic by the factor of $f/\bar{f}$, it also leads to a similar reduction below geostrophic in the tangential component at the boundary. Thus, our interpolation formula is consistent with other computational practices used in the forecast procedure.

A number of charts of this computed $\hat{\psi}_7$ have been produced as well as charts of wind speeds and directions computed from the $\hat{\psi}_7$ data. These wind charts were compared with actual analysed charts and with random wind observations at 700 mb. Also, several cases of winds computed from $\hat{\psi}_7$ fields were compared analytically with actual observations over North America. These experiments showed no significant difference between

average winds computed geostrophically from actual analyses and winds computed from the $\hat{\psi}_7$ fields.

After the $\hat{\psi}_7$ field has been determined, the local rate of change of the dewpoint depression T_d, at time τ is given by

$$\left(\frac{\partial T_d}{\partial t}\right)_\tau = -\frac{g}{\bar{f}} J[\hat{\psi}_7, T_d] + \gamma W_\tau \tag{2}$$

where $\bar{f}$ is the Coriolis parameter at 45° latitude, and g is the acceleration of gravity. Dewpoint depression changes due to vertical motion are assumed dry adiabatic in nature, and the vertical gradient of dewpoint depression is assumed to be locally zero. The coefficient γ is then the dry adiabatic rate of change of dewpoint depression, and is approximately equal to 8° C./km., depending on temperature and pressure. The vertical motion, W, at time τ is obtained by

$$W_\tau = \tfrac{1}{2}(W_{\tau-1} + W_{\tau+1}) \tag{3}$$

using one hour increments in τ. Centered differences in time are used for extrapolation of T_d, namely,

$$(T_d)_{\tau+1} = (T_d)_{\tau-1} + 2\left(\frac{\partial T_d}{\partial t}\right)_\tau \tag{4}$$

Negative values are not permitted.

Within the model there is a field of the altitudes of smoothed terrain. Using this terrain height field (z_s), the approximate surface stream function, $\hat{\psi}_s$ is determined at each point i, j by extrapolating from 500-mb. stream function data to the surface altitude as follows:

$$\hat{\psi}_{s_{i,j}} = \hat{\psi}_{5_{i,j}} - \left(\frac{z_5 - z_{s_{i,j}}}{z_5 - z_{8.5}}\right)_{\text{Std.Atm.}} \Delta z_{8.5-5_{i,j}} \tag{5}$$

Using $\hat{\psi}_s$ to determine the surface wind $\mathbf{V}_s$, the vertical motion at the surface due to terrain is given at each point by

$$w_{s_{i,j}} = (\mathbf{V}_s \cdot \nabla z_s)_{i,j} \tag{6}$$

It is probable that the decrease in the value of orographically induced vertical motions with height is nonlinear. Estoque [3] and Smebye [6] suggest that the factor $\left(\frac{p}{p_s}\right)^b$ suitably represents the decrease of orographic vertical motion with height, where p is pressure and p_s is the standard atmospheric pressure of the altitude at point i, j. b is taken here to be 2.5. The vertical motion at 700 mb. due to orographic effects is given approximately by

$$w_{0_{i,j}} = w_s\left(\frac{p_7}{p_s}\right)^{2.5}_{i,j} \tag{7}$$

The effect of the surface friction contribution to vertical motion was shown by Smagorinsky and Collins [5] using a relationship derived from Charney and from Brunt. The vertical motion at 700 mb. from surface friction w_f is given by

$$w_{f_{i,j}} = \left[\sqrt{\frac{K}{2f}} \sin(2\nu)\zeta_s\right]\left(\frac{p_7}{p_s}\right)^{2.5}_{i,j} \tag{8}$$

where K, the coefficient of eddy viscosity, is 10^5 cm./sec.; f is the Coriolis parameter; ν, the angle between the wind and isobars at the surface, is taken to be 22.5°; and ζ_s is the relative vorticity at the surface and is related to $\nabla^2\hat{\psi}_s$.

The final large-scale vertical motion used in the forecast is given by

$$W_{i,j} = w + w_0 + w_f \tag{9}$$

and is then used in (3).

3. OPERATION AND OUTPUT

The forecast change of the dewpoint field is computed in 1-hour time steps using the method outlined in the previous section. At the end of each time step, the Lewis nomogram table is entered to determine at which points large-scale precipitation is expected to occur. At these particular points, the temperature at 700 mb. is estimated from the forecast thickness value by the following simple relation (temperature in ° A.)

$$T_{7_{i,j}} = \left(\frac{T_7}{z_5 - z_{8.5}}\right)_{\text{Std.Atm.}} \Delta z_{8.5-5_{i,j}}$$

Smebye [6] has shown that the quantity of precipitation falling out of the atmosphere, assuming a pseudoadiabatic process, is related to the temperature at 700 mb. and the vertical motion. Therefore, if large-scale precipitation is indicated for a point, then the temperature at 700 mb. is estimated and, using the vertical motion forecast for the particular time step, a 1-hour precipitation quantity is determined for each point. These results are accumulated in a special field, and are printed out as a 24-hour quantitative precipitation forecast chart (fig. 4) at the end of the forecast.

At times 0, 12, 24, and 36 hours, the Lewis nomogram is entered and the cloud and large-scale precipitation parameter for each grid point is determined. This field is contoured with the following scheme:

(No symbol) ----	Less than 0.1 middle cloudiness.
$ ----------	0.1 to 0.5 middle cloudiness.
● ----------	0.5 through 1.0 middle cloudiness.
0 ----------	Area of active tropical shower activity and/or area of intermittent large-scale precipitation.
X ----------	Area of large-scale precipitation.

At the grid points are entered the forecast mean dewpoint depressions in tenths of degrees Celsius. It must be noted that this model is considered to depict only large-scale weather occurrence, since the mesh length of the grid used at JNWP is about 200 miles. Disturbances smaller in size than this may be lost within the grid.

The areas depicted by the "0's", and not appearing in the Lewis nomogram, are the result of an attempt at

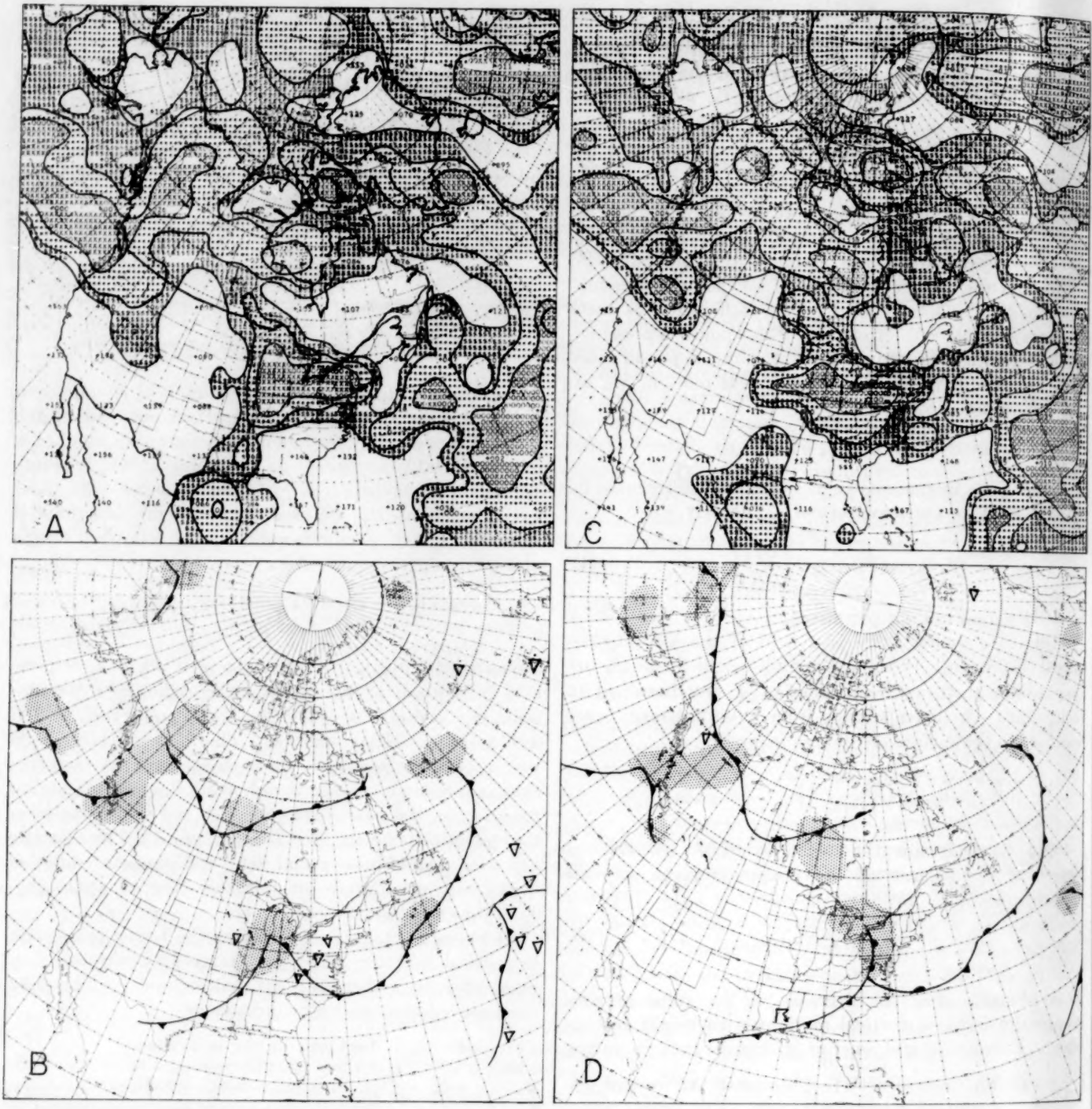

FIGURE 2.—(A) Initial chart of middle cloudiness and large-scale precipitation for 1200 GMT, April 28, 1959. Grid values are mean 850–700-mb. dewpoint depression in tenths of degrees C. See text for meaning of symbols. (B) Fronts and observed areas of precipitation for 1200 GMT, April 28, 1959, taken from the National Weather Analysis Center surface analysis chart. (C) 12-hour forecast middle cloudiness and large-scale precipitation area chart for 0000 GMT, April 29, 1959. (D) Observed frontal positions and precipitation areas for 0000 GMT, April 29, 1959. Note: Because of necessary reduction for printing, only a portion of the charts is shown. The forecast program produces charts covering the entire Northern Hemisphere to about 15° N.

showing areas of active tropical shower activity. Curtis and Panofsky [2] showed that there is a poor relationship between vertical motion computed from the thermotropic model and tropical air mass shower activity, including the afternoon shower activity over the United States in summer. They did find a good predictor of convective activity by considering the moisture present in the 900–700-mb. layer and the presence of a heated

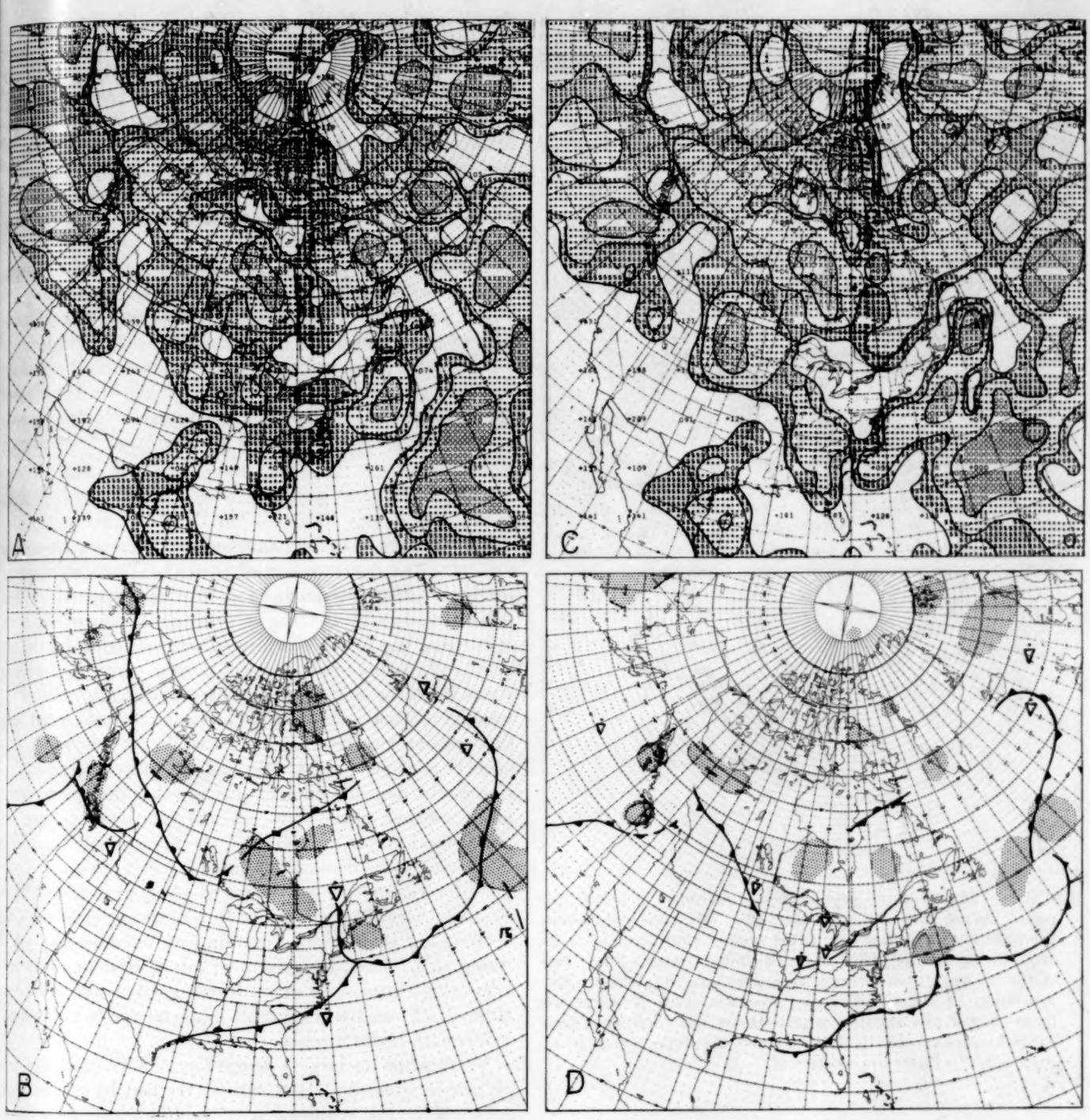

FIGURE 3.—(A) 24-hour forecast middle cloudiness and large-scale precipitation area chart for 1200 GMT, April 29, 1959. (B) Observed frontal positions and precipitation areas for 1200 GMT, April 29, 1959. (C) 36-hour forecast middle cloudiness and large-scale precipitation area chart for 0000 GMT, April 30, 1959. (D) Observed frontal positions and precipitation areas for 0000 GMT, April 30, 1959.

surface under a tropical air mass. On the assumption that this relation would obtain elsewhere over the hemisphere where tropical air is present over a heated surface, grid points over land masses for times during local afternoon and over sea areas having a mean sea surface temperature greater than 72° F. were listed. This list of points is contained within the program to "tag" the grid points where the shower predictor would obtain. After

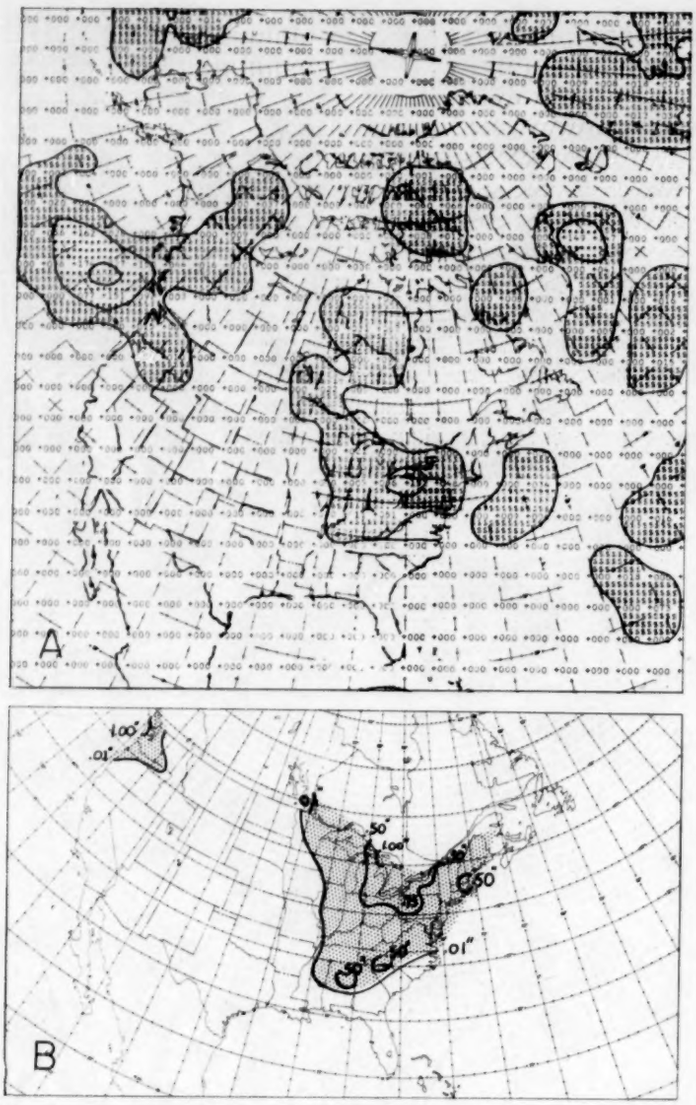

FIGURE 4.—(A) 24-hour precipitation quantity forecast for period ending 1200 GMT, April 29, 1959. (B) Observed 24-hour precipitation quantities for period ending 1200 GMT, April 29, 1959, in the area of the contiguous United States. Note: Precipitation quantities forecast here are those obtained by consideration of some large-scale processes only. Tropical air mass shower precipitation quantities are not considered here. Tropical shower activity is important and experiments to incorporate this factor are continuing.

the program computes the weather parameter for a point from the Lewis nomogram, the grid point list is consulted to determine if the point is "tropical." If so, the thickness field is consulted to see if the forecast value of the 850–500-mb. thickness is greater than an arbitrary value of 14,000 feet. If so, the forecast dewpoint depression value for the point is tested to see if the relative humidity is greater than 60 percent. If all these tests are passed, the probability of tropical shower activity is good and the parameter for tropical showers is stored for that point. It will be noted that all large-scale precipitation areas are surrounded by a band of "0" characters. This is due to an effect of the contouring program. The numerical value of showers for the contouring program must be chosen between cloudy and precipitation. Hence, when the program contours the large-scale precipitation areas, the areas are surrounded with spurious "0's". This is rationalized to be acceptable because precipitation is often intermittent or showery at the edges of an area.

The maps are printed on "onion skin" tracing paper which can be run through a reproducing machine with a plastic overlay of the geography superimposed. Examples of the forecast are shown in figures 2 through 4.

At present, the program nearly saturates the storage capacity of the IBM 704 computer. Within the limited space remaining, experiments are being conducted on ways of estimating the quantity of precipitation from shower activity.

4. LIMITATIONS

The limitations of a scheme such as described herein are several. The development of multi-level models is in its infancy. There is much room for improvement within these models and as these improvements are effected results from the forecast-of-precipitation-model should improve. It is believed that the largest error in forecasts stems from the errors in placement and magnitude of the vertical motion centers. This error is also associated with the present two-level model's inability to forecast true baroclinic development. Second, the forecast precipitation model depends upon empirical relationships to determine weather parameters. These relationships are not understood at present. Third, the precipitation model is not a true three-dimensional model but it is rather a one-level forecast with some degree of freedom in the vertical. Fourth, there is no allowance for obtaining moisture data from below the 850-mb. layer and we have no way yet of doing this. Last, the effects of latent heat of condensation where precipitation is forming have not been considered. Thus, there is ample material for future experiments with better models.

Verification is largely subjective. Although the precipitation quantity chart can be verified by comparison, such subjective verification of middle cloudiness is not simple often due to obscuration by low clouds and darkness. The verification of the forecast of dewpoint depressions for 24 hours is accomplished by machine. The machine computes the mean absolute error over the grid points encompassing the dense data network of North America. Insufficient verification data have been collected to date to permit a comprehensive objective verification. Activities of the Air Force, Navy, and Weather Bureau are receiving these charts by facsimile and local delivery and are evaluating them for usefulness.

To show the factor of machine speed over hand speed

for the same job, the following figures are presented: Lewis's technique takes about one-half hour to compute the forecast dewpoint depression spread for one station. The forecaster was forced to use charts 12 hours apart to compute the trajectory of the parcels. The present machine forecast technique produces a 36-hour dewpoint depression forecast for 1977 points using time steps of only 1 hour. This 36-hour forecast takes only 15 minutes, a gain factor of 35,586. In addition, the machine produces the forecast in map form along with auxiliary charts. Granting the crudeness of this forecast model, it is possible to foresee the time when electronic computers will actually forecast the meteorological parameters on an operational basis. This day may not be too far away.

ACKNOWLEDGMENTS

The author is deeply indebted to 1st Lt. Howard Potter, USAF, assigned to JNWP, who carried out the large task of programming and checking out this forecast model. The author is also indebted to Dr. G. P. Cressman, Director, JNWP, for his kind and helpful comments and suggestions; Dr. F. G. Shuman and other members of the JNWP Development Section for their collective comments and suggestions; and Major W. E. Lewis, USAF, and Capt. Earl Kindle, USAF, who provided much of the early inspiration.

REFERENCES

1. H. A. Bedient and G. P. Cressman, "An Experiment in Automatic Data Processing," *Monthly Weather Review*, vol. 85, No. 10, Oct. 1957, pp. 333–340.
2. R. C. Curtis and H. A. Panofsky, "The Relation Between Large-Scale Vertical Motion and Weather in Summer," *Bulletin of the American Meteorological Society*, vol. 39, No. 10, Oct. 1958, pp. 521–531.
3. M. A. Estoque, "A Graphically Integrable Prediction Model Incorporating Orographic Influences," *Journal of Meteorology*, vol. 14, No. 4, Aug. 1957, pp. 293–296.
4. W. Lewis, "Forecasting 700-mb. Dewpoint Depression by a 3-Dimensional Trajectory Technique," *Monthly Weather Review*, vol. 85, No. 9, Sept. 1957, pp. 297–301.
5. J. Smagorinsky and G. Collins, "On Numerical Prediction of Precipitation," *Monthly Weather Review*, vol. 83, No. 3, Mar. 1955, pp. 53–67.
6. S. J. Smebye, "Computation of Precipitation from Large-Scale Vertical Motion," *Journal of Meteorology*, vol. 15, No. 6, Dec. 1958, pp. 547–560.
7. P. D. Thompson and W. L. Gates, "A Test of Numerical Prediction Methods Based on the Barotropic and Two-Parameter Baroclinic Models," *Journal of Meteorology*, vol. 13, No. 2, Apr. 1956, pp. 127–141.

Weather Note

MEASUREMENT OF WIND SPEEDS NEAR A TORNADO FUNNEL

RESEARCH UNIT, U.S. WEATHER BUREAU, KANSAS CITY, MO.

[Manuscript Received July 8, 1959; Revised November 12, 1959]

On April 2, 1957, a tornado struck Dallas, Tex. During this storm at a site about 1,500 feet from the tornado path, Mr. Maurice Levy, a photographer for the National Broadcasting Co., took some excellent pictures with a 16 mm. movie camera exposing at 24 frames per second. In all, nearly 600 frames were exposed.

A Weather Bureau meteorologist from the Kansas City Research Unit later measured angles and distances at the Dallas site for use in computing distances and sizes of features shown in the pictures. The Research Unit enlarged the individual frames to 4-inch x 5-inch prints to facilitate the computations. One set of computations was made to study the horizontal motion of identifiable particles of debris, about the funnel vortex. Of these, 149 individual particles were considered large enough and could be traced long enough to yield significant measurements. Their movements were traced for periods in excess of 100 frames. The time interval covered was short enough that for all practical purposes the distance between camera and funnel could be taken to be constant. Each particle was identified on the prints involved, and the particle's apparent direction of motion, relative size, and instantaneous position relative to the vortex were recorded.

By trigonometry, the path of the particles was found to be about a circle of approximately 300 feet in diameter. Deviations did not exceed 10 percent. The speed of the particles was obtained by measurement of the distance traveled against the time involved. This distance traveled is defined as the apparent movement corrected for curvature of the path. The maximum speed obtained from this method was 212 miles per hour.*

It must be mentioned, however, that this is only the speed of a particle which does not necessarily reach the speed of the wind. The relation of the particle speed to the actual wind speed depends upon the aerodynamic properties of the particle itself, and this information is not available.

*Mr. Walter Hoecker of the Office of Meteorological Research, U.S. Weather Bureau, Washington, D.C., using another movie from another place along this tornado's path, obtained a rather close value, about 170 m.p.h. (personal communication).

New Weather Bureau Publication

Technical Paper No. 36, "North Atlantic Tropical Cyclones," Washington, D.C., 1959, 214 pp.; for sale by Superintendent of Documents, U.S. Government Printing Office, Washington 25, D.C. Price $1.00.

Charts show (A) tracks of all known tropical cyclones of tropical storm intensity (sustained winds of 39 m.p.h. or over) for each year 1886 through 1958; (B) tracks of tropical cyclones beginning in each 10-day period during the six months of maximum frequency, June through November, for the years 1886 through 1958; and (C) tracks of tropical cyclones beginning in each decade of years, 1891–1950, during the months of June, July, and November, and during each 10-day period in August, September, and October. A short text accompanies the charts.

THE RELATION OF MONTHLY FIRE OCCURRENCE IN GEORGIA TO MEAN MONTHLY VALUES OF WEATHER ELEMENTS[1]

DANIEL W. KRUEGER

Supervising Fire Weather Forecaster, U.S. Weather Bureau, Macon, Ga.

[Manuscript received August 31, 1959]

ABSTRACT

The monthly number of forest fires in Georgia from 1951 to 1958 is compared with the monthly mean values of weather elements to determine the relationship of fire danger severity to one or more of these elements. Although variations in human behavior unrelated to weather contribute to fire occurrence, a parameter composed of two of these weather elements, the relative humidity at 1330 EST and the maximum temperature, is found to be highly significant. This parameter is then used to estimate frequency of severe fire conditions from 1918 to 1951 when complete fire records were not maintained.

1. INTRODUCTION

Weathermen and foresters recognize the fact that certain weather elements exert considerable influence on the occurrence and consequent spread of forest fires. An objective means of relating monthly or seasonal forest fire danger to specific weather conditions is of value to fire control administrators. The fire danger meter now in general use in Georgia does this very well. When a sufficiently long period of data from this meter become available to compare with fire records, evaluation of Georgia's fire prevention efforts will be possible by the means Keetch [1] used in the Northeast.

A sufficiently large portion of Georgia has been under State fire protection since 1951 so that fire records from State-protected lands are considered representative of fire conditions for the entire State. Continuity in fire danger station records, however, exists for only a short portion of this time. During this period, the danger meters were changed from type 5 to type 8, many stations were changed from the woods to the open type, a change in wind reduction tables was made, and there were the normal changes in locations and exposures.

If a parameter based on weather observations from regular Weather Bureau Offices could be found, it would be useful at least until a long period of continuous fire danger station observations become available. In addition such a parameter might provide a reliable means of predicting prolonged periods of severe fire danger based on previous experience since weather records are available for a much longer period of time than fire records. This analysis was, therefore, made to find such a parameter: one that had continuity of record, was readily obtainable, had a good correlation with actual fire hazard from a statistical point of view, and was related physically to the burning process.

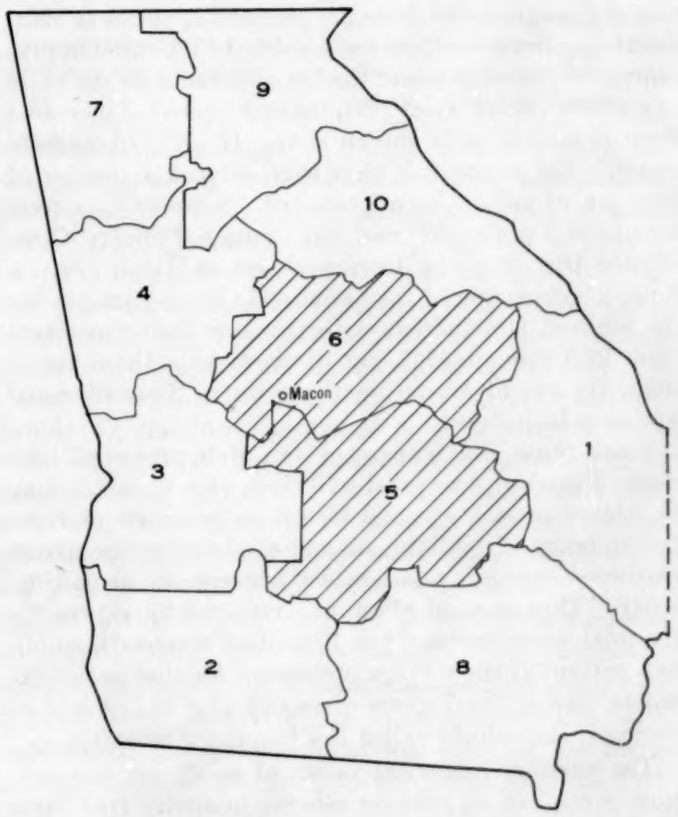

FIGURE 1.—Georgia Forestry Commission Districts. Note the location of Macon in relation to the 5th and 6th districts.

[1] A preliminary report of this study was presented at the Second National Conference on Agricultural Meteorology, 170th National Meeting of the American Meteorological Society, October 22–24, 1958, in New Haven, Conn.

532363—60——3

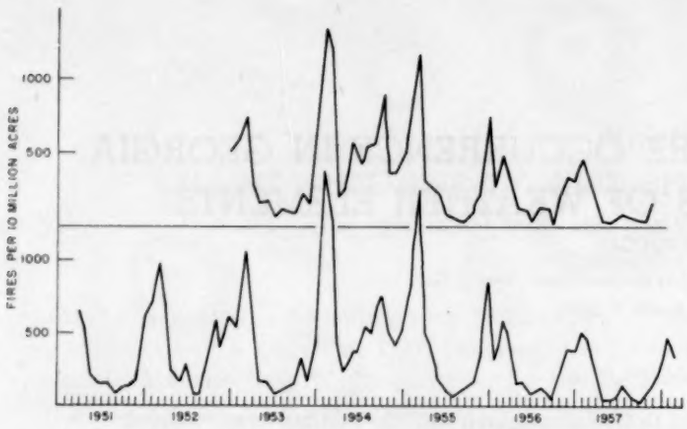

FIGURE 2.—Monthly fire occurrence per 10 million acres protected, for State of Georgia (lower) and 5th and 6th Districts (upper).

2. PROCEDURE

Data used in this study were monthly fire records of the Georgia Forestry Commission and monthly weather data from the annual issues of *Local Climatological Data* for Macon, Ga., the Weather Bureau Office closest to the center of the State and, therefore, assumed to be most representative of the State as a whole.

Fire occurrence records appear to be reliable for the 7-year period April 1951 through March 1958, for that portion of Georgia under State fire protection. Prior to 1951, the area under protection was considered too small to give representative estimates of the fire occurrence for the State as a whole. Since April 1951, the area protected increased from 14 million to 22 million acres. In order to compare monthly fire occurrences, they were reduced to number of fires per 10 million acres protected. Similiar data were calculated for the 5th and 6th Georgia Forestry Commission Districts—the districts closest to Macon (fig. 1). Since a comparison of the variation in fire occurrence for the 5th and 6th districts with that for the entire State from 1953 through 1957 (fig. 2) shows only minor variations, the use of Macon weather data in State comparisons may be justified.

Total State fire occurrence on State-protected land shows a marked seasonal distribution (fig. 3) which may be related to such seasonal factors as greenness of vegetation, hours of daylight, amount of shade (primarily in hardwood stands), and seasonal changes in human activity. This seasonal effect was removed by expressing the total fire occurrence per 10 million acres each month as a percent of the average occurrence for that particular month during the 7 years of record (fig. 4). For convenience, this will be called fire frequency hereafter.

The monthly numerical values of maximum temperature, precipitation, 1330 EST relative humidity (the value closest to the minimum of those available), wind speed, percent of possible sunshine, and number of days with 0.01

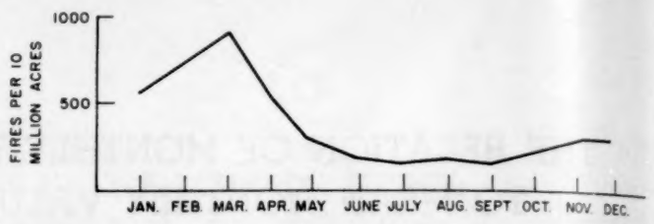

FIGURE 3.—Monthly average fire occurrence per 10 million acres protected, for State of Georgia during period April 1951 through March 1958.

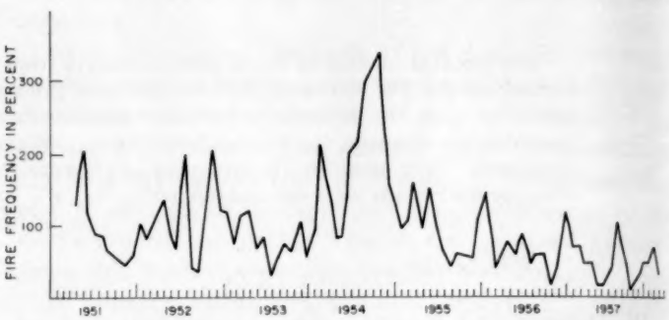

FIGURE 4—Monthly fire frequency for State of Georgia, expressed as a percent of the average for that month for the 7-year period 1951 to 1958.

inch or more of precipitation, as found in *Climatological Data* for Macon, were compared with numerical values of fire frequency. Other data available either were not considered to be related to the physical burning process or were essentially a duplication of the above data. For example, cloudiness would be related to sunshine and consequently was not included.

Seasonal effects were removed from the weather data by expressing the value of each weather element as the deviation from its average value for that month during the 7-year period of record. Hereafter, this will be referred to as deviation of maximum temperature, deviation of 1330 EST relative humidity, etc.

3. RESULTS

The deviation of 1330 EST relative humidity from the average was found to be most closely related to the fire frequency. Since relative humidity is related to fuel moisture, this relationship to fire frequency is what would be expected from physical reasoning. Because the scatter diagram (fig. 5) indicated a non-linear relationship, the regression equations for fire frequency vs. the logarithm, the inverse, and the square of the deviation from average relative humidity were computed. These variables were all significant at the 1 percent level. The inverse and the square were about equally significant, and both were considerably better than the logarithmic and the linear forms. When the equations were plotted on the scatter diagram the inverse curve appeared to give a better fit than the

square in the area of high fire frequency. Thus the inverse curve was selected (fig. 5).

The residuals from this equation were then plotted against the deviations of each of the other weather elements. The relationship between the residual and maximum temperature was found to be significant at the 1 percent level. A multiple regression analysis was then computed for fire frequency using monthly deviations of maximum temperature and the inverse of the monthly deviations of relative humidity as the independent variables.

The residuals from this new equation were plotted against the remaining weather readings but no significant relationship could be found. Sunshine is closely related to maximum temperature and somewhat related to humidity, so these elements apparently already took care of any contribution sunshine could make. Average wind is so strongly influenced by high speeds in a few storms that the average value may be meaningless as a criterion of average weather conditions. Also, while wind is physically related to the spread of fire, its relationship to ignition is much less pronounced. Precipitation has only a brief effect upon the moisture content of some of the lighter fuels; even after a heavy rain in the morning, fires often start quite easily in the afternoon. Precipitation would have a noticeable effect, therefore, only if it occurred sufficiently near the time of daily minimum fuel moisture to keep the fuel moisture from reaching its usual low. These early afternoon rains are more than likely reflected in the 1330 EST relative humidity and the maximum temperature. Precipitation also varies so much over short distances that the Macon precipitation may not have been representative of average conditions over the State (both relative humidity and maximum temperature vary far less from place to place).

The final regression equation was

$$F=-31.74+\frac{2393.02}{H+20}+5.32T$$

where F is fire frequency in percent of the monthly average for the 7-year period, H is the deviation of 1330 EST relative humidity from the monthly average, and T is the deviation of maximum temperature from the monthly average. The multiple correlation coefficient was 0.83 which indicates that approximately 69 percent of the variation was accounted for by the two variables H and T. In view of the variation unaccounted for, the equation may have more value in dividing fire danger into broad categories such as severe, average, and low, than in determining specific fire danger values for each month. Arbitrarily, severe conditions were defined as those in which monthly fire frequency was greater than 150 percent of the 7-year monthly average, and low fire danger was defined as fire frequency less than 50 percent of the

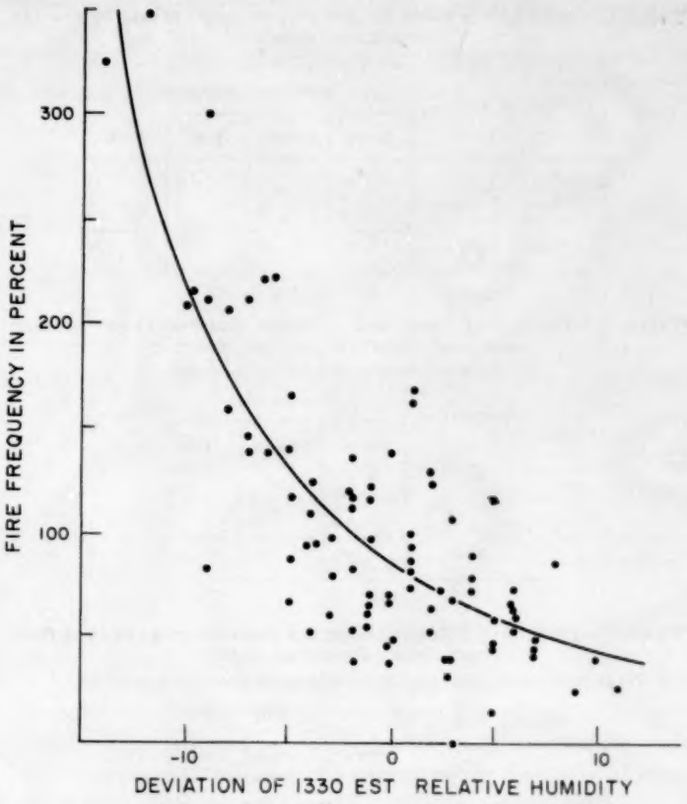

FIGURE 5.—Scatter diagram of monthly fire frequency vs. deviation from average monthly 1330 EST relative humidity. The curve shows the best-fitting inverse relation of fire frequency to deviation of relative humidity.

monthly 7-year average. Tables 1, 2, and 3 show the results of applying the equation and these definitions to the dependent data. The estimates from this equation for the three categories of fire frequency are 82 percent correct with a skill score [2] of 0.62. It is evident that the results are better on severe cases than on low cases, which was noted in selecting the inverse rather than the square of the humidity in forming the equation. If only two classes are used, severe and not severe (average and low combined), the forecasts are 95 percent correct with a skill score of 0.81. Severe fire conditions occurred in 13 months during the period; severe fire conditions would have been forecast for 10 of these 13 months. In one other month severe fire weather conditions would have been forecast, but they did not occur (table 4).

The equation has been tested on independent data from the period April 1958 through July 1959. Figure 6 shows both the scatter of these data and the results of dividing these data into the three classes. The skill score on the independent data was 0.46 for the three classes. In general, fire danger was low through most of

[2] Skill score is defined as $(R-E)/(N-E)$ where R is the number of correct forecasts, N is the total number, and E is the number expected to be correct from chance. See Brier and Allen [2].

TABLE 1.—*Contingency table for fire frequency forecasts by months (dependent data)*

Observed fire frequency	Forecast fire frequency			
	Severe	Average	Low	Total
Severe	10	3	0	13
Average	1	52	2	55
Low	0	9	7	16
Total	11	64	9	84

TABLE 2.—*Percent of time each forecast class occurred in each observed class (dependent data)*

Observed class	Forecast class		
	Severe	Average	Low
Severe	91	5	0
Average	9	81	22
Low	0	14	78
Total	100	100	100

TABLE 3.—*Percent of time each observed class occurred in each forecast class (dependent data)*

Observed class	Forecast class			
	Severe	Average	Low	Total
Severe	77	23	0	100
Average	2	95	3	100
Low	0	56	44	100

TABLE 4.—*Months when severe fire weather was forecast, observed, and both forecast and observed (dependent data except 1958)*

Year	Months											
	Jan.	Feb.	Mar.	Apr.	May	June	July	Aug.	Sept.	Oct.	Nov.	Dec.
	Classification											
1951	—	—	—	—	B	—	—	—	—	—	—	—
1952	—	—	—	—	—	—	B	—	—	—	O	—
1954	—	B	F	—	—	B	B	B	B	B	O	—
1955	—	—	B	—	O	—	—	—	—	—	—	—
1956	B	—	—	—	—	—	—	—	—	—	—	—
1958	—	—	—	—	—	—	—	—	—	—	B	—

F=forecast but not observed.
O=observed but not forecast.
B=forecast and observed.

this period. It is felt that a higher skill score would be likely in a sample containing more severe months. The one month of severe fire weather conditions was correctly indicated by the equation.

4. DISCUSSION

A nomogram (fig. 7) was constructed from the equation and used to determine the months of severe fire weather in Georgia since 1918 (table 5). The fall of 1927 and almost all of 1954, known as bad fire periods, were indicated severe by the formula. Two or more consecutive severe fire months are rare, but as many as five

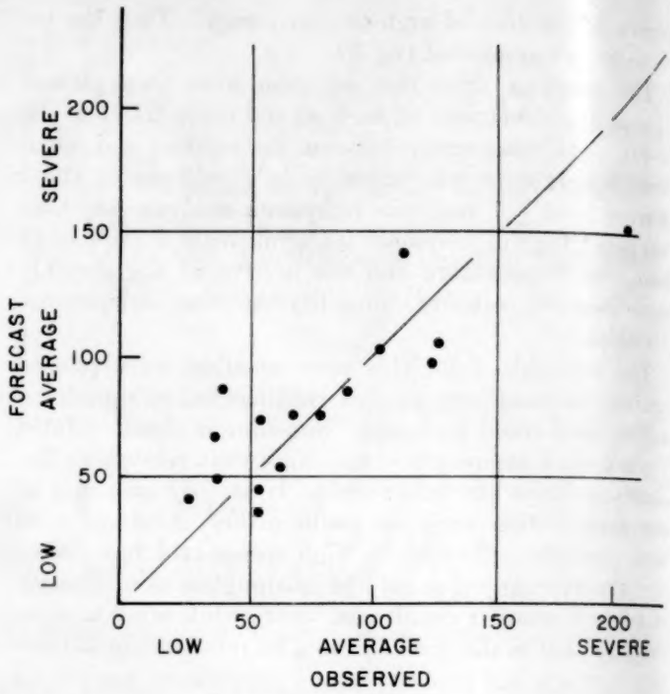

FIGURE 6.—Observed fire frequency vs. forecast fire frequency (independent data).

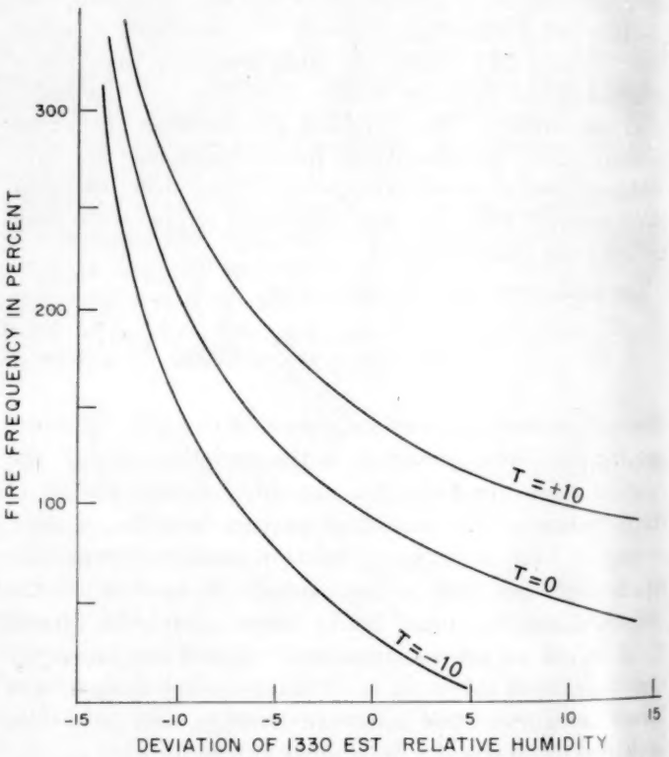

FIGURE 7.—Monthly fire frequency in percent of the average vs. deviation of 1330 EST relative humidity from the monthly average. Curves represent deviations of maximum temperatures of −10°, 0°, and +10° from the average.

TABLE 5.—*Months of severe fire weather in Georgia since 1918, as determined by monthly relative humidity and maximum temperature deviations*

Year	Jan.	Feb.	Mar.	Apr.	May	June	July	Aug.	Sept.	Oct.	Nov.	Dec.	Total	Consecutive months	Years without severe periods
1918	—	—	x	—	—	—	—	—	—	—	—	—	1		
1919	—	—	—	—	—	—	—	—	x	—	—	—	1		1
1921	—	—	—	—	—	—	—	—	x	—	—	—	1		
1922	—	—	—	—	—	—	—	—	x	—	—	—	1		2
1925	—	—	x	—	—	—	—	—	x	—	—	—	2		1
1927	—	—	—	—	—	—	—	—	x	x	—	—	2	2	2
1930	—	x	—	—	—	—	—	—	—	—	—	—	1		
1931	—	—	—	—	—	x	—	—	—	—	—	—	1		
1932	—	—	x	—	—	—	—	—	—	—	—	—	1		3
1936	—	—	x	—	—	—	—	—	—	—	—	—	1		1
1938	—	—	—	—	—	—	—	—	—	x	—	—	1		2
1941	—	—	—	—	x	—	—	—	—	—	—	—	1		
1942	—	—	—	x	—	—	—	—	—	—	—	—	1		
1943	—	x	—	—	—	—	—	—	—	—	x	—	2		2
1946	—	x	—	—	—	—	—	—	—	—	—	x	2		
1947	—	x	—	—	—	—	—	—	—	—	—	—	1		3
1951	—	—	—	—	x	—	—	—	—	—	—	—	1		
1952	—	—	—	—	—	—	x	—	—	—	—	—	1		1
1954	—	x	x	—	—	x	x	x	x	x	—	—	7	2 and 5	
1955	—	—	x	—	—	—	—	—	—	—	—	—	1		
1956	x	—	—	—	—	—	—	—	—	—	—	—	1		1
1958	—	—	—	—	—	—	—	—	—	—	x	—	1		
Total	1	5	6	1	2	2	2	1	6	3	2	1	32	9	19

x=severe fire weather.

consecutive severe months have occurred. Severe conditions have occurred in all seasons but are most frequent in late summer and early autumn, and again in late winter. Over half (22 out of 41) of the years had at least one severe month. The longest consecutive number of years free of severe conditions was 3.

The physical relationship of these variables to fire occurrence appears logical. Fuel moisture, of course, varies directly with relative humidity and determines to a considerable degree the ease with which a forest fire may start. Temperature, on the other hand, has an inverse effect on fuel moisture and at high temperatures the fuel is closer to its kindling point.

These preliminary checks indicate that relative humidity and temperature deviations apparently account for a considerable portion of the variation in fire occurrence in Georgia for the period for which actual data are available. The residual may be partially accounted for by the fact that Macon weather is not always representative of that for the State as a whole. A much larger portion, however, is probably due to non-weather factors. From Davis's [3] summary, it is seen that 97 percent of Georgia fires are man-caused, and many are of incendiary origin. Although weather may control how often man's carelessness results in fire, it does not control how often man is careless. Education, fuel reduction, new fire laws, and other fire prevention efforts are generally conceded to have reduced the number of fires during recent years, but it is difficult to estimate the exact amount of reduction without an objective measure of weather influence.

5. CONCLUSIONS

Conclusions from this study, of course, are tentative and based only on the period and area for which data were used. They should be checked with data from other areas of Georgia as well as from surrounding States. The tentative conclusions are:

1. Fire frequency in Georgia is more closely related to humidity and temperature than to other weather elements, such as wind, sunshine, amount of precipitation, and frequency of precipitation.

2. The regression equation obtained in this study is usable to obtain past occurrences of severe fire conditions.

3. The equation may be of value in removing the effect of weather from fire records to evaluate success in fire prevention, assuming, of course, that the variation not accounted for is largely due to non-weather causes.

4. If in the future, long-term forecasts of average maximum temperature and minimum humidity (similar to the Weather Bureau's present 30-day mean temperature and rainfall predictions) become available, the equation may be of value to forewarn of severe fire conditions.

REFERENCES

1. John J. Keetch, "Occurrence Rate as a Measure of Success in Fire Prevention," *Fire Control Notes*, vol. 18, No. 1, 1957, pp. 41–45.

2. Glenn W. Brier and R. A. Allen, "Verification of Weather Forecasts," *Compendium of Meteorology*, American Meteorological Society, Boston, 1951, pp. 841–848.

3. Kenneth P. Davis, *Forest Fire Control Problems and Research Needs in Georgia*, Georgia Forestry Commission, 1956.

THE WEATHER AND CIRCULATION OF OCTOBER 1959

A Predominantly Cold, Wet Month in the United States

ROBERT H. GELHARD

Extended Forecast Section, U.S. Weather Bureau, Washington, D.C.

1. SOME FEATURES OF THE GENERAL CIRCULATION

The 700-mb. circulation in the western Northern Hemisphere during October 1959 was characterized by a complete cycle in the 5-day mean zonal index at middle latitudes. Figure 1 shows that the zonal index reached a minimum during the 5 days centered October 5, rose steadily to a peak value of 12.8 meters per second in the period centered on October 19, and then declined rapidly again to below normal values during the last week of the month.

Despite this cycle, the long-wave pattern remained remarkably persistent during the month. The most persistent feature was the deep trough in the central Pacific (fig. 2) which fluctuated only slightly about its mean position. The low center in this trough moved gradually northward during the month as the blocking which dominated the first, or low-index, half of the month retrograded from the Bering Sea to the Kamchatka Peninsula. This evolution is shown in figure 3, the 15-day mean 700-mb. circulation for each half of October.

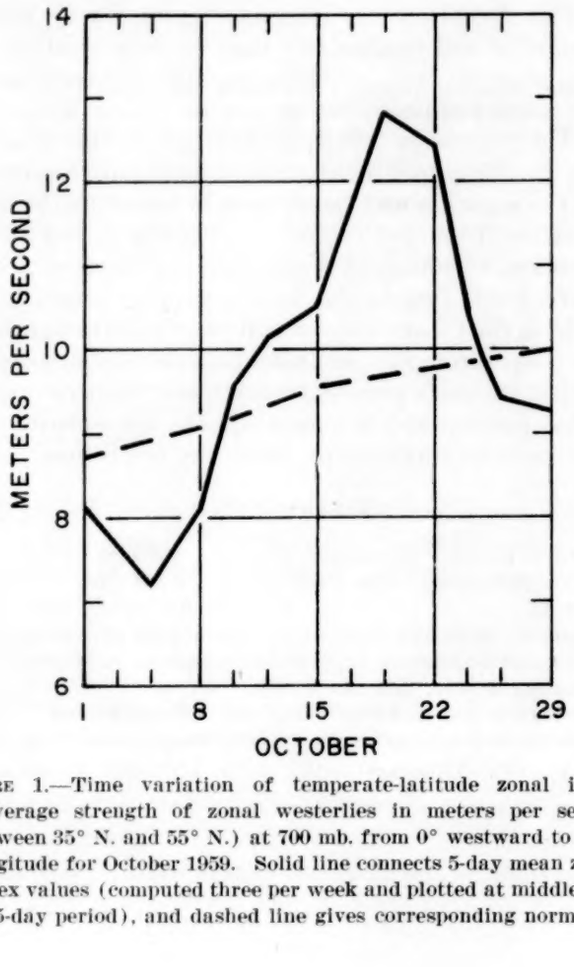

FIGURE 1.—Time variation of temperate-latitude zonal index (average strength of zonal westerlies in meters per second between 35° N. and 55° N.) at 700 mb. from 0° westward to 180° longitude for October 1959. Solid line connects 5-day mean zonal index values (computed three per week and plotted at middle day of 5-day period), and dashed line gives corresponding normal.

Figure 3 also shows that slow eastward progression of the ridge near the northwestern coast of North America and the trough downstream in the central United States occurred from the first to the second half of the month as the zonal index increased. More striking was the change in anomalous flow along the west coast of North America, as shown by the dotted lines in figure 3. The meridional character of this flow during the first half of the month was representative of the northerly steering which carried very cold air over the Middle and Far West. By contrast, in the latter half of the month the northerly component of the anomalous flow shifted from the area of the Continental Divide to the Mississippi Valley, bringing cold air into the eastern half of the United States.

As might be expected in view of the persistent long-wave pattern, the cycle in the zonal index was largely related to changes in amplitude. However, the rapid increase in index around mid-month was not accompanied by rapid progression of the trough and its associated cold air in the central United States. A regional breakdown of the hemispheric zonal index to include only the continental portion between 55° W. and 125° W. reveals little change between the half-monthly and full-monthly indices. For this area the mean zonal index for October 1–15 was 9.1 m.p.s.; for October 16–30, 8.8 m.p.s.; and for October 1–30, 9.0 m.p.s. During the first half of the month, when the zonal index for the western Northern Hemisphere was lowest, the mean index over North America at middle latitudes was highest. It is obvious, therefore, that the major changes in the strength of the westerlies must have occurred in the oceanic areas. This is clearly seen in the northward shift of negative 700-mb. height anomalies in the mid-Pacific and mid-Atlantic, as shown by the 15-day mean 700-mb. charts (fig. 3).

In Europe during October the general circulation underwent the first great change since May 1959 when a strong blocking High became established over the British Isles [1]. For six months 700-mb. heights averaged above normal in northwestern Europe as a center of positive anomaly oscillated between southern Scandinavia and Great Britain along the track shown in figure 4.

As a corollary, it may be noted that during this period the Bermuda portion of the Atlantic subtropical High was dominant, while the Azores portion, when evident, existed only at low latitudes. The result was a predominant southerly wind component in the eastern Atlantic, as typified by figures 1 and 2A, and warm dry weather in the British Isles and western Europe [2]. In sharp contrast, figure 2B shows the Azores portion of the Atlantic subtropical High well above normal near Spain with a strong

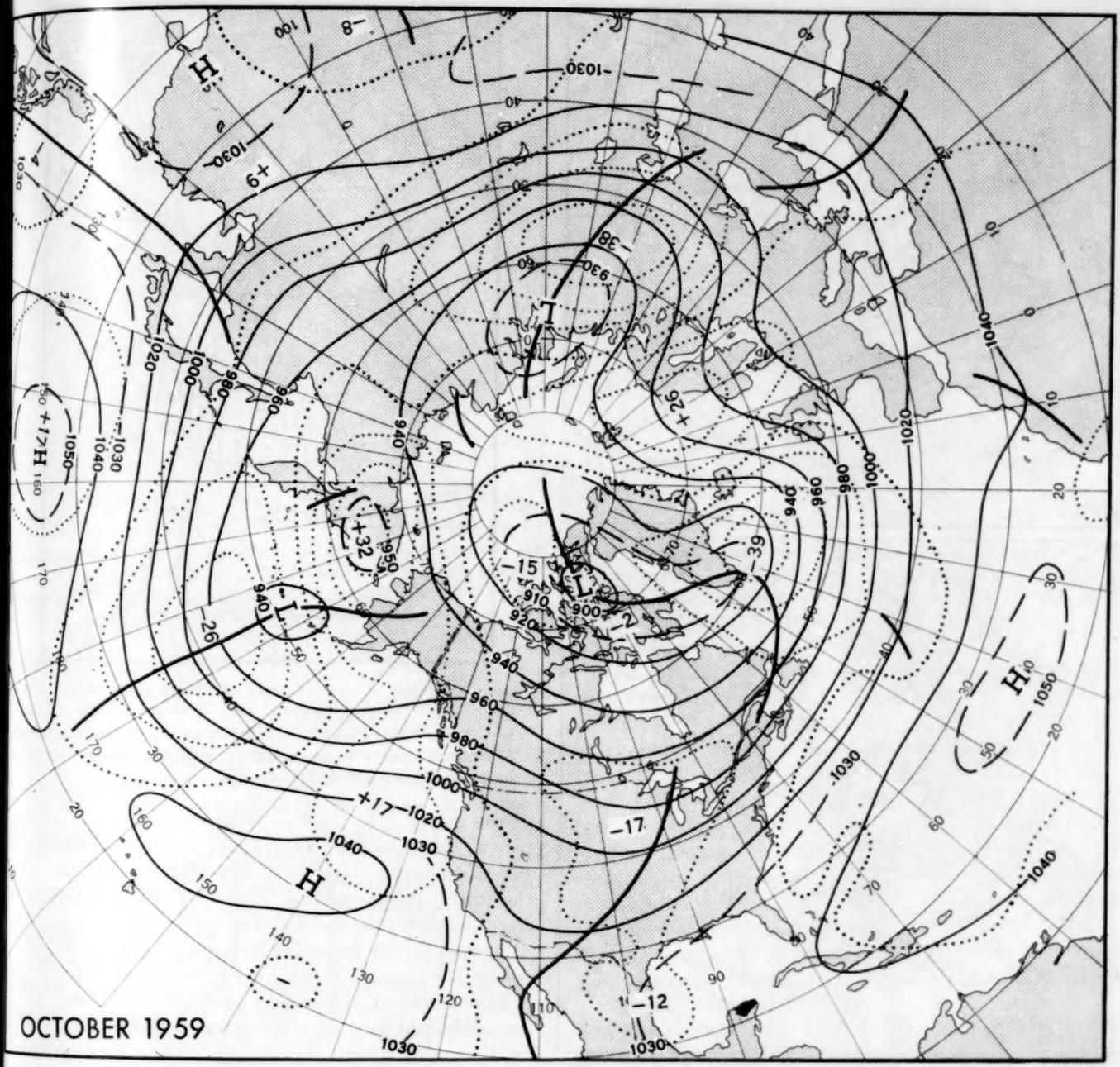

FIGURE 2.—Mean 700-mb. height contours and departures from normal (both in tens of feet) for October 1959. Deep mid-Pacific vortex and blocking to the north were important factors influencing North American weather.

land of confluence between it and the Icelandic Low. This configuration was associated with fast westerlies across northern Europe as shown by figure 3B, more in the manner suggested by the axis of maximum 700-mb. wind speed on the normal for October (given by the dashed line in fig. 5). This change is more dramatically highlighted by the difference in 700-mb. height anomaly between the first and second halves of October, as much as −920 feet in the Norwegian Sea and +630 feet in the northeastern Atlantic (fig. 6).

It should be noted that blocking was still a dominant feature of the circulation at high latitudes during the second half of October, as shown by the +310-ft. height anomaly (fig. 3B) near Novaya Zemlya. It would appear at first glance that blocking had merely progressed from the Norwegian Sea. However, since the migration of blocking is usually a retrogressive process, it is more likely that part of the blocking in the Bering Sea mentioned earlier (fig. 2A) retrograded toward northern Russia. It is also possible that this blocking surge was enhanced initially by warm air advection from the northeastern Atlantic into the Arctic during the first half of the month.

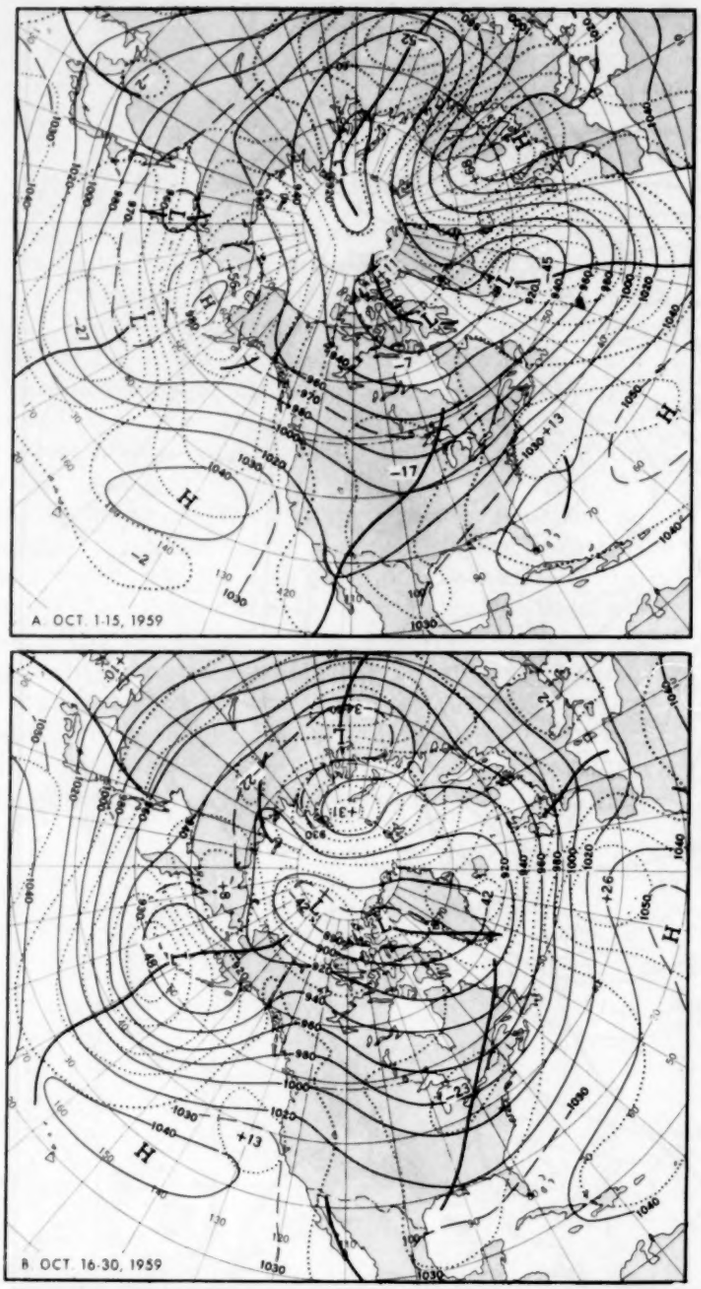

FIGURE 3.—Fifteen-day mean 700-mb. height contours and departures from normal (both in tens of feet) for (A) October 1–15, 1959, and (B) October 16–30, 1959.

2. WEATHER IN THE UNITED STATES

TEMPERATURE

The temperature regime over the contiguous States of the United States during October 1959 was characterized by a slow eastward migration in the anomaly picture throughout the month, as highlighted by a series of weekly temperature anomaly maps (fig. 7). These show a more or less uniform advance as colder than normal air masses invaded farther eastern positions with a gradual increase in temperature anomaly in the West and a decrease in the East. Below normal temperatures prevailed throughout most of the month in the central half

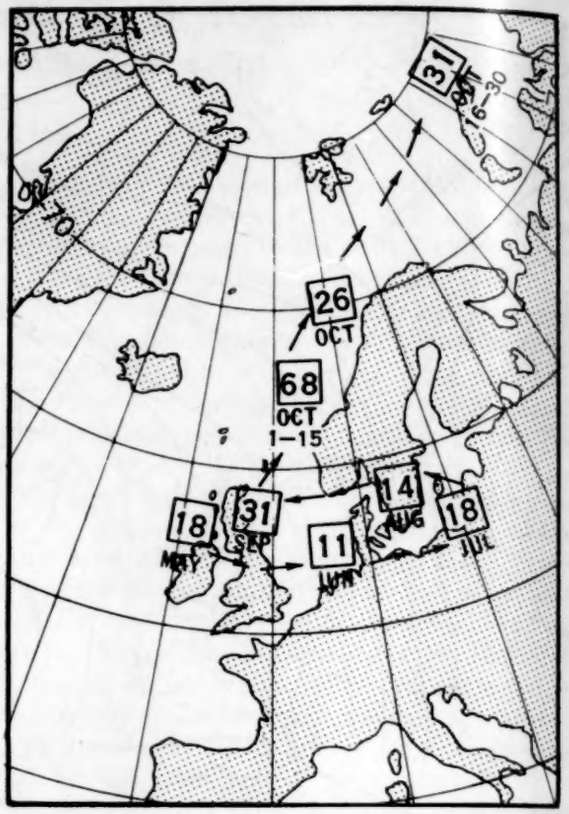

FIGURE 4.—Position and intensity of 30-day mean center of positive 700-mb. height anomaly over western Europe from May to October 1959, including 15-day mean anomalies for October. Number in square is the height anomaly in tens of feet for the month indicated below it.

of the nation. In the Far West the increase in temperature to the degree shown in figure 7D was associated with persistent anticyclonic conditions aloft in that area. After the initial polar outbreak (fig. 7A), Pacific anticyclones were dominant as the 700-mb. ridge-trough system (fig. 3) moved slowly eastward, bringing warm air masses into the West and cold polar air progressively farther east.

In the central and eastern parts of the country the abnormally cold weather was related in part to the unusually cold air mass source region near Hudson Bay. Although mean 700-mb. heights were only slightly below normal in this area, the thickness of the layer between 1000 and 700 mb. averaged considerably below normal for the month (fig. 8). In addition, in the eastern half of the country, the maximum westerlies were well south of their normal position (fig. 5), allowing migratory cyclones to introduce frequent outbreaks of polar air from central Canada. Note how perturbations from the Pacific (fig. 9) were steered around the periphery of the cold dome, generally following a path just north of the axis of maximum 700-mb. wind speed (fig. 5).

The pattern of 700-mb. height departure from normal for the month (fig. 2) appears well correlated with the monthly mean temperature anomaly pattern (fig. 10A), except in the East and Southeast where heights were

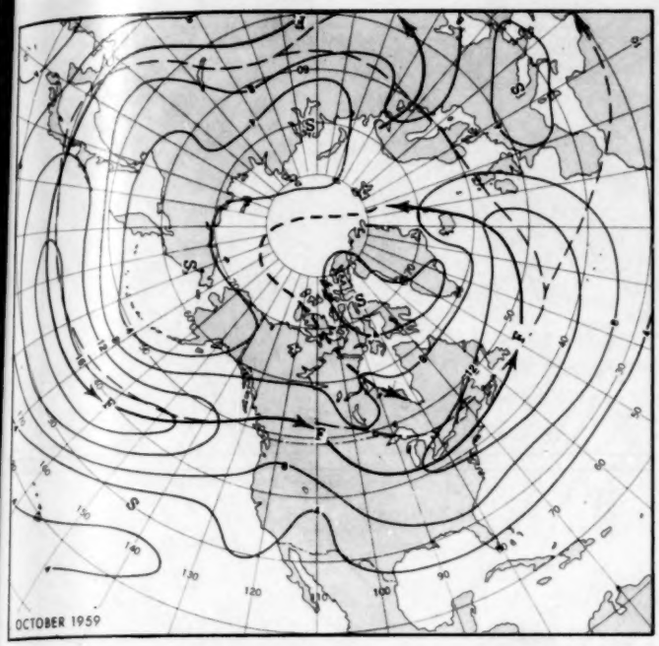

FIGURE 5.—Mean 700-mb. geostrophic wind speed (meters per second) for October 1959. Heavy solid lines indicate primary axis of 700-mb. jet stream, and thin, dashed lines the normal October position. "F" and "S" designate wind speed maxima and minima. Note the secondary jet around the polar vortex indicated by the heavy, dashed arrow.

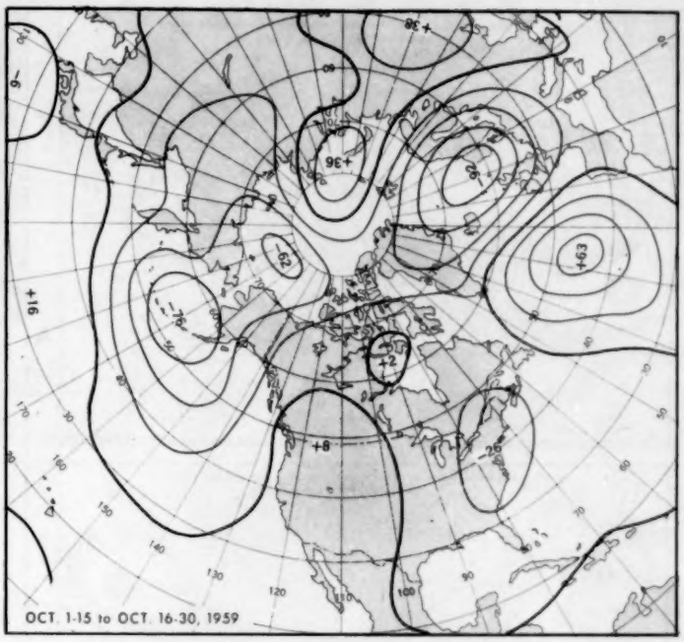

FIGURE 6.—Change in 700-mb. height anomalies (tens of feet) from October 1–15 to October 16–30, 1959. Areas of greatest change were in northern Pacific and western Europe, where relaxation of blocking occurred.

slightly below normal but temperatures above normal. However, this apparent discrepancy can be related to the southerly anomalous flow, advecting warm air masses from the Gulf of Mexico intermittently throughout the period.

Locally, October proved to be a month of extreme weather throughout the contiguous United States. Early in the month, while the Middle and Far West were establishing low temperature records for early fall, daily records for maximum temperatures were being broken from the Ohio Valley to New England (fig. 7A). In the central portion of the country, where below normal temperatures persisted throughout the month, Milwaukee, Wis. had its second coldest October on record, and Topeka, Kans. reported the coldest October in 35 years. By the end of the month new daily minimum records were being established in the Northeast (fig. 7E) while many new daily maximum records, in excess of 90 degrees, were reported in Arizona, New Mexico, Nevada, and California.

PRECIPITATION

Precipitation was normal or above throughout the country except in California and Nevada, where little or none fell (fig. 10B). Light precipitation fell in a belt from Washington and Oregon eastward to South Dakota. Subsidence associated with persistent anticyclonic conditions and maintenance of a storm track well to the north combined to produce the record dryness in California and Nevada and resulted in an extension of the forest fire season. Several fires were raging near Eureka, Calif. at the end of the month.

Most of the excess precipitation occurred along the slowly moving boundary of sharply contrasting air masses, particularly in the southern Great Plains and the Southeastern States. The quasi-stationary character of much of the frontal activity involved is shown by figure 11, the number of days with fronts during the month. A line connecting the maxima, from the northern Great Basin southeastward through Texas to the Gulf of Mexico and then northeastward to southern New England, outlines the mean boundary of the cold air. In addition, two tropical storms contributed additional rainfall from Florida to North Carolina, causing extensive flooding in the Carolinas where general rains had already produced considerable amounts.

When one considers that October is normally a fair, dry month for most of the United States, the precipitation records established become more spectacular. Record amounts of precipitation in Texas, Oklahoma, and Kansas ranged from 11.38 inches at Dallas, Tex. to 6.37 inches at Concordia, Kans. From New Orleans, La. to Norfolk, Va., precipitation records for October were broken. Representative amounts which set new records are 12.09 inches at Apalachicola, Fla. and Columbia, S.C., 9.60 inches at Greensboro, N.C., and 9.39 inches at Macon, Ga.

In southern New England record daily precipitation, such as 4.45 inches at Hartford, Conn. on October 23–24, was responsible for flood conditions on the Connecticut River. As in New England, frontal rains set new precipitation records for October at Marquette and Sault Ste. Marie, Mich., and near records at Milwaukee, Wis. and Detroit, Mich.

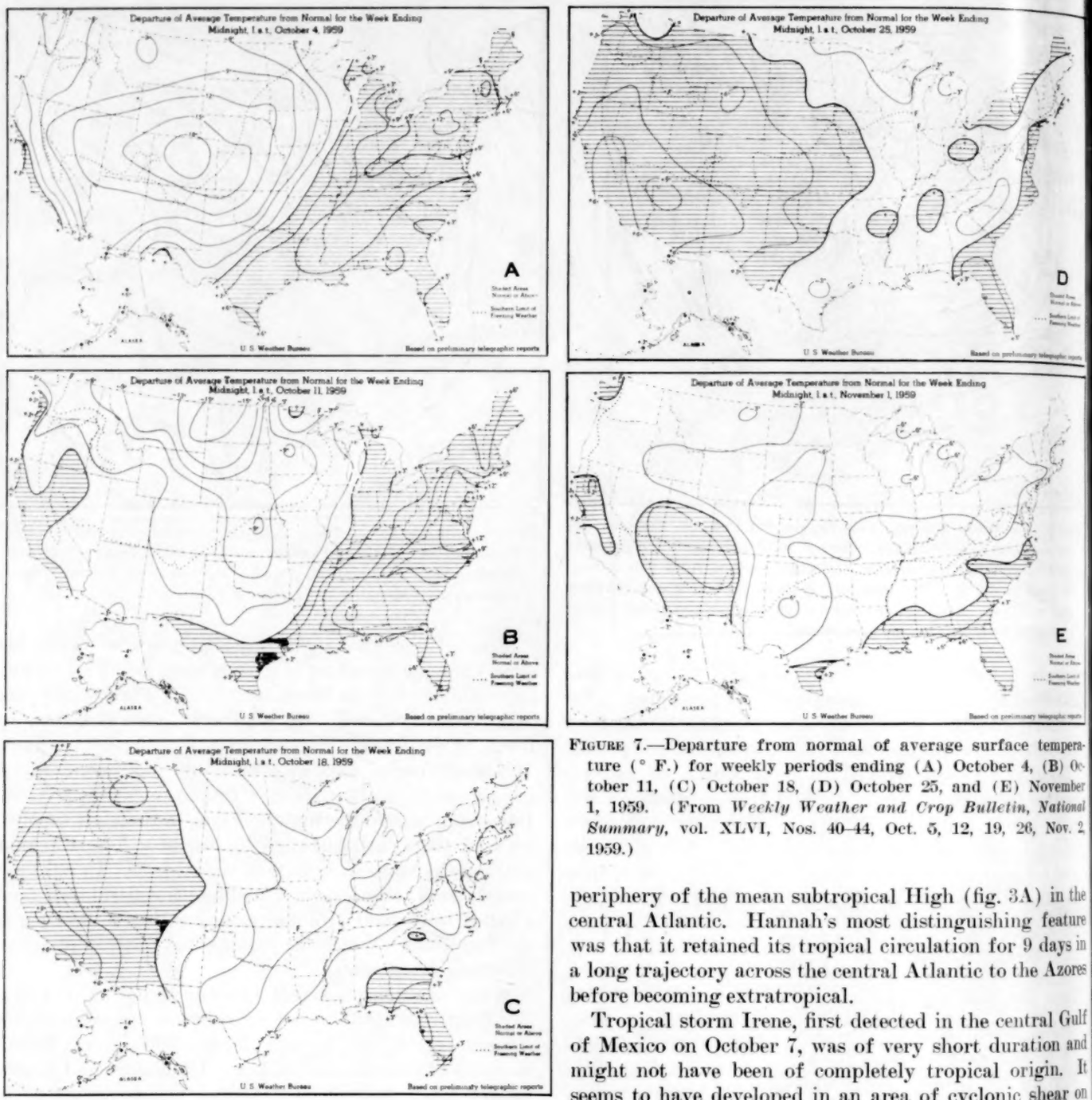
Departure of Average Temperature from Normal for the Week Ending
Midnight, l.s.t., October 4, 1959
A
U.S. Weather Bureau
Departure of Average Temperature from Normal for the Week Ending
Midnight, l.s.t., October 25, 1959
D
U.S. Weather Bureau
Departure of Average Temperature from Normal for the Week Ending
Midnight, l.s.t., October 11, 1959
B
U.S. Weather Bureau
Based on preliminary telegraphic reports
Departure of Average Temperature from Normal for the Week Ending
Midnight, l.s.t., November 1, 1959
E
U.S. Weather Bureau
Based on preliminary telegraphic reports
Departure of Average Temperature from Normal for the Week Ending
Midnight, l.s.t., October 18, 1959
C
U.S. Weather Bureau
Based on preliminary telegraphic reports

FIGURE 7.—Departure from normal of average surface temperature (° F.) for weekly periods ending (A) October 4, (B) October 11, (C) October 18, (D) October 25, and (E) November 1, 1959. (From *Weekly Weather and Crop Bulletin, National Summary*, vol. XLVI, Nos. 40–44, Oct. 5, 12, 19, 26, Nov. 2, 1959.)

3. TROPICAL STORM ACTIVITY

ATLANTIC

Three tropical storms developed during October in widely scattered areas, one east of the Leeward Islands, one in the central Gulf of Mexico, and one in the western Caribbean Sea. Their tracks are shown in figure 12A.

The major storm, Hannah, first observed near 21° N., 57° W. on September 29, moved rapidly northwestward to about 200 miles west of Bermuda by 0000 GMT of October 2. It then recurved, following a path around the periphery of the mean subtropical High (fig. 3A) in the central Atlantic. Hannah's most distinguishing feature was that it retained its tropical circulation for 9 days in a long trajectory across the central Atlantic to the Azores before becoming extratropical.

Tropical storm Irene, first detected in the central Gulf of Mexico on October 7, was of very short duration and might not have been of completely tropical origin. It seems to have developed in an area of cyclonic shear on a stationary front extending from Illinois to the central Gulf of Mexico. Simultaneous with the origin of Irene was the development of a deep Colorado Low which brought a fresh outbreak of polar air into the lower Mississippi Valley. This reduced Irene to a weak extratropical wave on the polar front within 48 hours, but not before it had produced heavy rains, particularly in northwestern Florida and in Georgia.

Tropical storm Judith was first detected as a tropical depression between Yucatan and Cuba on October 17. According to Haggard [3] and others, there is a definite maximum of tropical storm development in the western

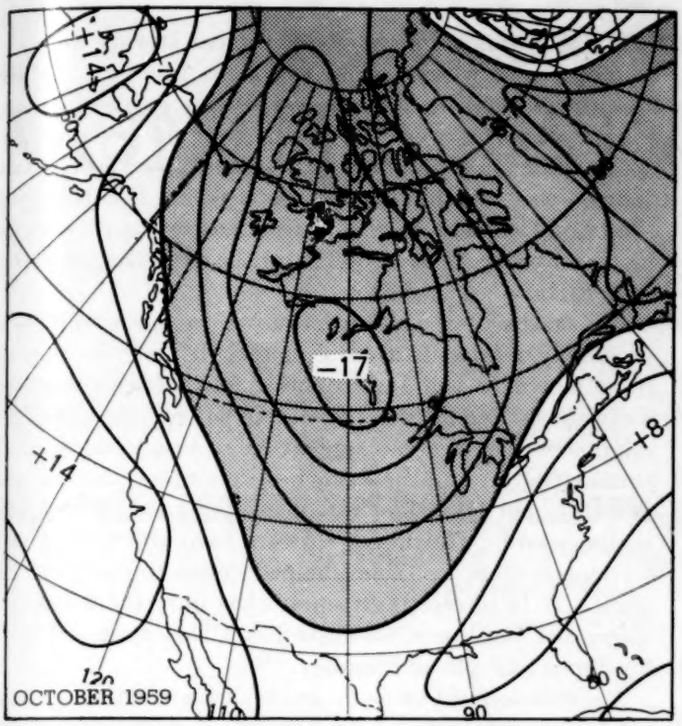

FIGURE 8.—Departure from normal of mean thickness (1000–700 mb.) for October 1959, with subnormal values shaded. Isoline interval is 50 feet, and centers are labeled in tens of feet.

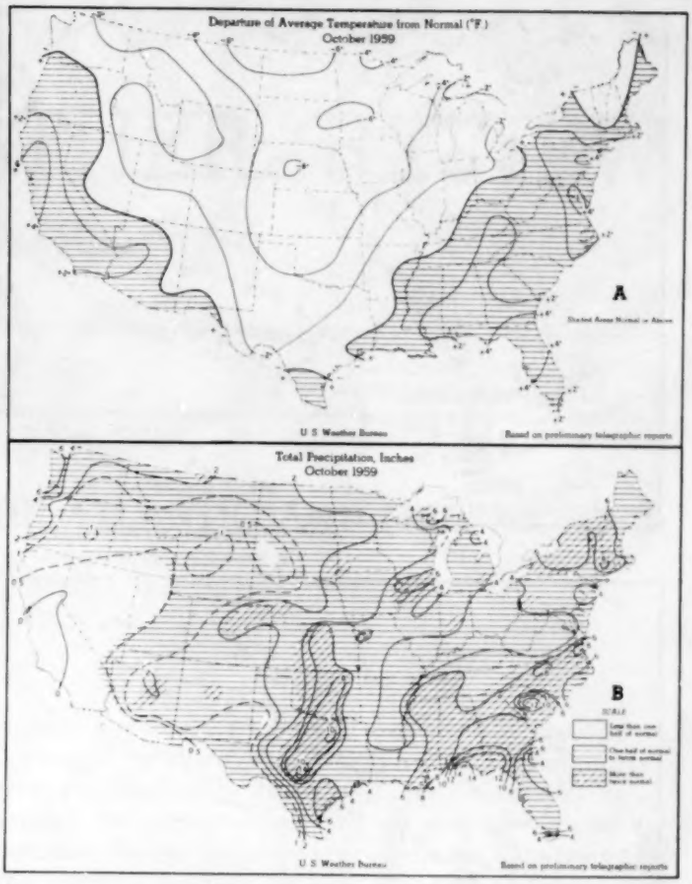

FIGURE 10.—(A) Monthly mean surface temperature departure from normal (° F.), and (B) total precipitation (inches), both for October 1959. (From *Weekly Weather and Crop Bulletin, National Summary*, vol. XLVI, No. 44, Nov. 2, 1959.)

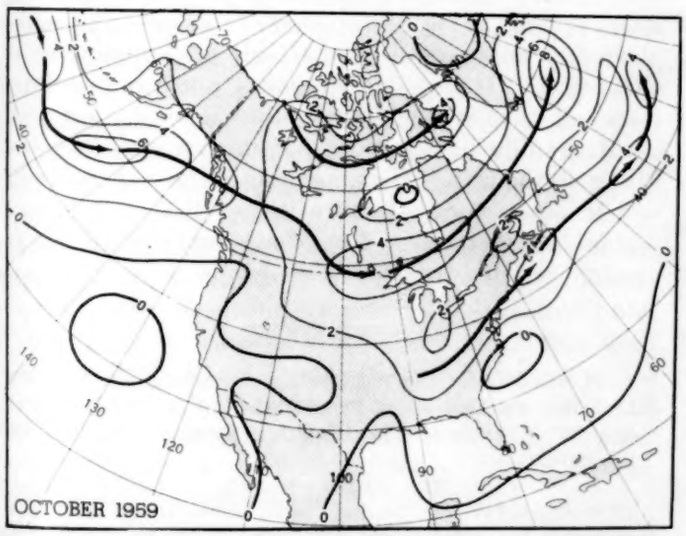

FIGURE 9.—Frequency of cyclone passages (within 5° squares at 45° N.) during October 1959. Well-defined cyclone tracks are indicated by solid arrows.

FIGURE 11.—Number of days in October 1959 with fronts of any type within unit squares (with sides approximately 500 miles). All frontal positions are taken from *Daily Weather Map*, 1:00 p.m., EST. Areas with fronts on 15 or more days are stippled. Quasi-stationary fronts were frequent in the Great Basin and the northeastern Gulf of Mexico.

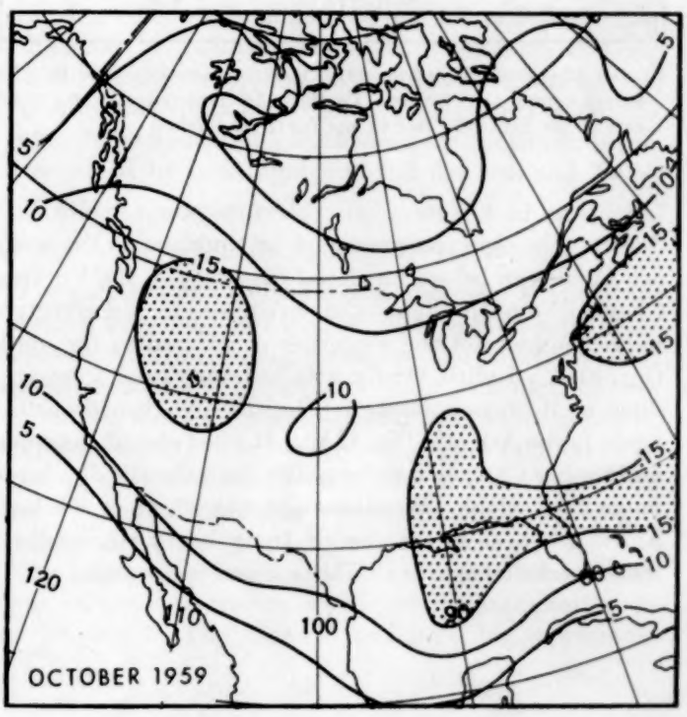

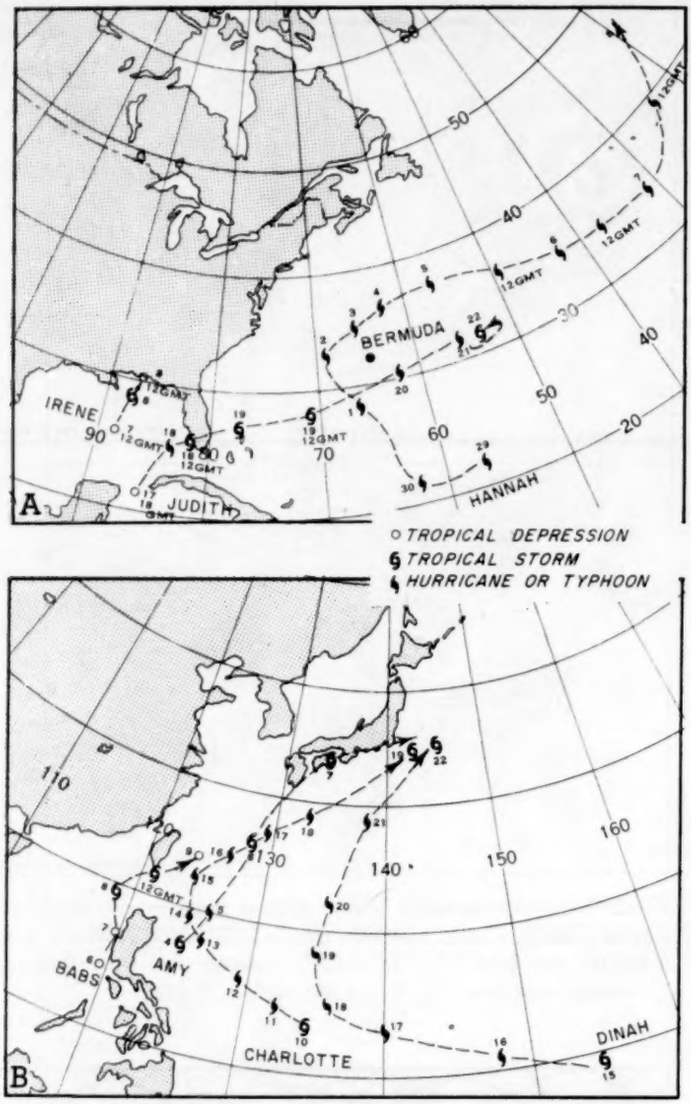

FIGURE 12.—Tropical storm activity during October 1959 in (A) Atlantic and (B) western Pacific. All positions are for 0000 GMT on the date indicated except for those marked.

Caribbean in October. It therefore seems likely that Judith existed in some stage of development in the western Caribbean before its official discovery in the Yucatan Channel. Judith might have developed into a destructive hurricane had not the westerlies penetrated so far south (fig. 2B). Judith briefly attained hurricane intensity, filled as it crossed southern Florida, and then deepened again in the Atlantic (fig. 12A). It filled east of Bermuda on October 22 when it came under the influence of a large polar anticyclone. Wind damage was slight in southern Florida, but, as in the case of Irene, heavy rains caused some flood damage in the Lake Okeechobee area.

PACIFIC

In the western Pacific four tropical storms were observed, two of which attained typhoon intensity. Three of these storms threatened the southern coast of Japan, but the westerlies were close to their normal position (fig. 5) and farther south than in September, when typhoon damage was very heavy [2]. As a result, the damaging effects of October's storms were decreased as they weakened and became extratropical off the east coast of Japan (fig. 12B).

The tracks of these storms shown in figure 12B were all closely related to the mean trough position (fig. 2) from Korea to the Philippines. Mean conditions over the western Pacific were favorable to tropical storm development; i.e., the subtropical ridge was stronger than normal (fig. 2) and the easterlies were more than 4 m.p.s. above normal (not shown). Conditions for recurvature, as discussed by Hawkins [4], were favorable throughout the month (figs. 2, 3) and helped define the mean storm track. It is interesting to note that only those tropical storms originating in the easterlies, Charlotte and Dinah, developed to typhoon intensity.

A discussion of October's tropical storm activity would not be complete without mention of the destructive storm that struck the west coast of Mexico near Manzanillo, causing widespread damage from heavy rains, high tides, and flash floods. Unfortunately, all analyses of this storm must be deduced from scattered ship reports. This storm appears to have originated as a tropical depression about 250 miles south of the Gulf of Tehuantepec on October 22. It then moved slowly northwestward and deepened until it reached hurricane intensity just south of Manzanillo on the 27th, before moving inland and filling on the 28th. Here, as in Japan in September [2] and in other cases of severe loss of life from tropical storms [5], destruction from floods and disease was far greater than that from hurricane winds.

REFERENCES

1. C. M. Woffinden, "The Weather and Circulation of May 1959—Including an Analysis of Precipitation in Relation to Vertical Motion," *Monthly Weather Review*, vol. 87, No. 5, Sept. 1959, pp. 196–205.
2. J. F. O'Connor, "The Weather and Circulation of September 1959—Quasi-Periodic Oscillations in Zonal Index and Centers of Action," *Monthly Weather Review*, vol. 87, No. 9, Sept. 1959, pp. 357–366.
3. W. H. Haggard, "The Birthplace of North Atlantic Storms," *Monthly Weather Review*, vol. 86, No. 10, Oct. 1958, pp. 397–404.
4. H. F. Hawkins, Jr., "The Weather and Circulation of September 1956—Including a Discussion of Hurricane Flossy and September's Typhoon Tracks," *Monthly Weather Review*, vol. 84, No. 9, Sept. 1956, pp. 336–342.
5. I. R. Tannehill, *Hurricanes*, 9th Rev. Ed., Princeton University Press, 1956, 308 pp.

U.S. GOVERNMENT PRINTING OFFICE 19